

**Ab Initio Calculation of Atomic Ground State Energies using the In-Medium
Similarity Renormalization Group**

David Livermore

B.Eng, Carleton University

A thesis submitted to McGill University in partial fulfillment of the requirements of the
degree of
Master of Science

Physics Department
McGill University, Montréal

August 14, 2019

Copyright © 2019 David Livermore, All rights reserved.

Abstract

Computational many-body physics presents one of the most difficult challenges for theoretical physics. In order to solve many-body physics problems, we consider several choices of basis functions, and describe how to determine matrix elements in each basis for the atomic Hamiltonian evolved in the In-Medium Similarity Renormalization Group. Our results demonstrate that the Laguerre basis functions demonstrate an excellent basis, and we are able to calculate ground state energies of several Noble gases with extreme precision. The results of this research can further be built upon to create a tool for prediction of both nuclear and atomic physics properties *ab initio*.

Abstrait

Résoudre un problème à N corps s'avère être un des plus grands défis en physique théorique. Pour résoudre un tel problème, nous considérons plusieurs choix de fonctions de base et décrivons comment déterminer les éléments de l'Hamiltonien de l'atome dans chaque base après que celles-ci aient été évoluées à l'aide du "In-Medium Similarity Renormalization Group". Nos résultats montrent que la base des fonctions de Laguerre est un excellent choix. De plus, nous avons pu calculer l'énergie de l'état fondamental de plusieurs gas nobles avec une très grande précision. Les résultats de cette recherche peuvent servir d'assise pour la création d'un outil pouvant prédire tant les propriétés nucléaires qu'atomiques *ab initio*.

Dedication

To mum and dad; thanks for helping me out through thick and thin.

Author Contribution Statement

All calculations in this thesis were done by me using either code that I wrote myself or code that I adapted from Ragnar Stroberg. Ragnar Stroberg also assisted with the derivation of eqn. 3.9, Takayuki Miyagi assisted with the derivation of eqn. 3.16. Antoine Belley assisted in the translation of my abstract into french.

Acknowledgements

I want to thank Ragnar Stroberg for providing the base code from which I worked, as well as Takayuki Miyagi for his mathematical insights and keen eye for debugging, Antoine Belley for his assistance translating my abstract and Jason Holt for his support, insight and supervision throughout this project. I would also like to thank Thomas Brunner for accepting me as a graduate student and for advising me during my time as his graduate student.

Contents

1	Introduction and Motivation	11
2	Atomic Hamiltonian and Basis functions	13
2.1	Hydrogen-like basis	13
2.2	Harmonic Oscillator Basis	14
2.2.1	One-body Energy of Harmonic Oscillator	16
2.3	Laguerre Basis	16
2.4	Truncation Parameter	19
3	Electron-Electron Interaction	21
3.1	Many-Body Quantum Mechanics	21
3.2	Hydrogen-Like and Laguerre Bases	23
3.3	Harmonic Oscillator Basis	27
4	IM-SRG	30
4.1	Hartree-Fock Method	30
4.1.1	Variational Principle	31
4.1.2	Hartree-Fock Method	31
4.1.3	Limitations of the Hartree-Fock Method	32
4.2	In-Medium Similarity Normalization Group	33
4.3	Normal-Ordering and Wick's Theorem	34
5	Extrapolation methods	38
5.1	Least Squares	38

5.2	Exponential Fitting functions	39
6	Calculation Method	42
6.1	Harmonic Oscillator Basis Two-Body	43
6.2	Laguerre Basis Two-Body	43
7	Results and Discussion	45
7.1	Harmonic Oscillator Basis	45
7.2	Laguerre Basis	48
8	Conclusion & Future Work	59

List of Figures

4.1	Evolution of the Hamiltonian matrix with respect to the flow parameter. . .	35
5.1	Extrapolation of the ground state energy of helium as a function of the truncation parameter, E_{max} , using an exponential fit.	40
5.2	Extrapolation of the ground state energy of helium as a function of the truncation parameter, E_{max} , using a Gaussian fit.	41
7.1	Expectation of the ground state energy of helium, omitting the interaction between electrons as a function of the harmonic oscillator energy, $\hbar\omega$, and the truncation parameter, E_{max} . Blue indicates the lowest E_{max} , at $E_{max}=4$, increasing in increments of 4 while purple indicates the highest, at $E_{max}=16$.	46
7.2	Expectation of the ground state energy of helium, omitting the interaction between electrons as a function of the truncation parameter, E_{max} , using an exponential fit.	47
7.3	Expectation of the ground state energy of helium, omitting the interaction between electrons as a function of the truncation parameter, E_{max} , using a Gaussian fit.	48
7.4	Gaussian extrapolation of the ground state energy of helium as a function of the truncation parameter, E_{max}	49
7.5	Exponential extrapolation of the ground state energy of helium as a function of the truncation parameter, E_{max}	50

7.6	Expectation of the ground state energy of helium, omitting the interaction between electrons as a function of the length parameter, b and the truncation parameter, E_{max} , Blue indicates the lowest E_{max} , at $E_{max}=2$, increasing in increments of 2 while pink indicates the highest, at $E_{max}=6$	51
7.7	Expectation of the ground state energy of helium, omitting the interaction between electrons as a function of the length parameter, b and the truncation parameter, E_{max} ; examining the region about $b=2$, Blue indicates the lowest E_{max} , at $E_{max}=2$, increasing in increments of 2 while pink indicates the highest, at $E_{max}=6$	52
7.8	Hartree-Fock and IM-SRG calculations of the ground state of helium as a function of the truncation parameter, E_{max} , and the length parameter, b , including the Coulomb interaction between the electrons. Blue indicates the lowest E_{max} , at $E_{max}=2$, increasing in increments of 2 while pink indicates the highest, at $E_{max}=6$	53
7.9	Hartree-Fock and IM-SRG calculations of the ground state of helium as a function of the truncation parameter, E_{max} , and the length parameter, b , including the Coulomb interaction between the electrons examining the region around $b=2$. Dark blue indicates $E_{max}=2$, cyan is $E_{max}=4$, increasing in increments of 2, with purple being the highest at $E_{max}=12$	54
7.10	Hartree-Fock and IM-SRG calculations of the ground state of Neon as a function of the truncation parameter, E_{max} , and the length parameter, b . Dark blue indicates $E_{max}=2$, cyan is $E_{max}=4$, increasing in increments of 2, with purple being the highest at $E_{max}=12$	55
7.11	Hartree-Fock and IM-SRG calculations of the ground state of argon as a function of the truncation parameter, E_{max} , and the length parameter, b . Dark blue indicates $E_{max}=2$, cyan is $E_{max}=4$, increasing in increments of 2, with purple being the highest at $E_{max}=12$	56

7.12	Hartree-Fock and IM-SRG calculations of the ground state of krypton as a function of the truncation parameter, E_{max} , and the length parameter, b . Dark blue indicates $E_{max}=2$, cyan is $E_{max}=4$, increasing in increments of 2, with purple being the highest at $E_{max}=12$	57
7.13	Hartree-Fock and IM-SRG calculations of the ground state of xenon as a function of the truncation parameter, E_{max} , and the length parameter, b . Dark blue indicates $E_{max}=2$, cyan is $E_{max}=4$, increasing in increments of 2, with purple being the highest at $E_{max}=12$	58

Chapter 1

Introduction and Motivation

There are few fields of science as computationally demanding as many-body physics. In years past, *ab initio* methods have been too computationally demanding, limiting calculations in nuclear physics to lightest nuclei[1]. In this thesis, one particular approach known as In-Medium Similarity Renormalization Group (IM-SRG) will be discussed. IM-SRG takes the atomic many-body Hamiltonian matrix and evolves it with a unitary transformation [2]. This allows a decoupling of lower energy states from higher energy states, and reduces the computation difficulty associated with diagonalizing the Hamiltonian dramatically.

IM-SRG has found applications in numerous fields including nuclear physics (see e.g. [3, 1]), as well as evaluation of quantum dots [4, 5], here we discuss the application of IM-SRG specifically towards the analysis of ground state energies of atomic nuclei.

Although the current version of the code being used can only accommodate closed-shell systems, work is currently underway to extend the code to accommodate all of the other atoms, but for the purpose of this thesis, all of the results will focus on the noble gases, helium, neon, argon, xenon, and krypton.

Atomic physics, well studied since the early days of quantum mechanics, provides a fertile testing ground for certain nuclear properties, such as the charge radius of the nucleus [6, 7]. In order to make such determinations, extremely precise theoretical calculations of the atomic properties must be carried out. Experimental techniques, such as collinear laser spectroscopy, are able to measure numerous nuclear properties, including spin, charge radii and dipole moments, by making precise measurements of atomic properties [8].

If we consider the nucleus to infinitely small with infinite mass, and zero kinetic energy, then the non-relativistic kinetic energy of and coulomb force between the nucleus and an electron is simply

$$T = \frac{p^2}{2m_e}, \quad (1.1)$$

$$V = \frac{-Z\hbar c\alpha}{r}. \quad (1.2)$$

Where m_e is the mass of an electron, p is the momentum operator, Z is the number of protons in the nucleus, \hbar is the reduced Planck constant, α is the fine structure constant, c is the speed of light, and r is the distance of the electron from the nucleus. If, however, we consider a nucleus, which is still stationary, but has some finite mass, m_N , and is a sphere of uniform charge with radius R , then these operators become [9, 10]:

$$T = \frac{p^2}{2\mu}, \quad (1.3)$$

$$\mu = \left(\frac{1}{m_e} + \frac{1}{m_N} \right)^{-1}, \quad (1.4)$$

$$V = \begin{cases} \frac{-Z\hbar c\alpha}{2R} \left(3 - \frac{r^2}{R^2} \right), & \text{if } r < R \\ \frac{-Z\hbar c\alpha}{r} & \text{otherwise.} \end{cases} \quad (1.5)$$

One can then calculate the spectra for multiple values of R , compare to experimental results, and using the calculated results, estimate the radius of the nucleus. For the purpose of this thesis, we will first determine a suitable set of basis functions assuming a stationary nucleus with zero charge radius as in equations 1.1 and 1.2.

Chapter 2

Atomic Hamiltonian and Basis functions

2.1 Hydrogen-like basis

The atomic Hamiltonian for an atom with N electrons, Z protons and a total reduced mass of μ , can be well-represented by a simple Coulomb interaction between each electron and the nucleus, as well as another coulomb interaction between each pair of electrons (see e.g. [11]).

$$H = \sum_i^N T_i + \sum_i^N V_i + \sum_{i<j}^N V_{ij}. \quad (2.1)$$

Where T_i denotes the kinetic energy (eqn. 2.2), V_i denotes the Coulomb interaction between the nucleus and the i th electron (eqn. 2.3) and V_{ij} denotes the Coulomb interaction between the i th and j th electrons (eqn. 2.4).

$$T_i = \frac{p_i^2}{2m_e}, \quad (2.2)$$

$$V_i = -\frac{Z\hbar c\alpha}{r_i}, \quad (2.3)$$

$$V_{ij} = \frac{\hbar c\alpha}{|\vec{r}_i - \vec{r}_j|}. \quad (2.4)$$

Where $|\vec{r}_i - \vec{r}_j|$ is the distance between the i^{th} and j^{th} electrons, all other notation follows that given in chapter 1, eqns 1.1 and 1.2.

For the case of an atom with Z protons and a single electron (e.g. H, He⁺, Li⁺², etc.), we can simplify the equation by eliminating the two-body interaction (eqn. 2.4) and reduce the sums down to single terms (eqn. 2.5).

$$H = \frac{p^2}{2\mu} - \frac{Z\hbar c\alpha}{r}. \quad (2.5)$$

It can be shown (see e.g., [9]), that the eigenfunctions of this operator are:

$$\Psi_{nlm}(r, \theta, \phi) = R_{nl}(r)Y_{lm}(\theta, \phi), \text{ with} \quad (2.6)$$

$$R_{nl}(r) = \sqrt{\left(\frac{2Z}{na_\mu}\right)^3 \frac{(n-l-1)!}{2n[(n+l)!]} e^{\frac{-Zr}{na_\mu}} \left(\frac{2Zr}{na_\mu}\right)^l L_{n-l-1}^{2l+1}\left(\frac{2Zr}{na_\mu}\right)}. \quad (2.7)$$

Where Y_{lm} are spherical harmonics, L are associate Laguerre Polynomials, and a_μ is the reduced Bohr radius, given below

$$a_\mu = \frac{m_e a_0}{\mu} = a_0 \frac{m_A + m_e}{m_A}. \quad (2.8)$$

Where m_e is the mass of the electron and m_A is the mass of the nucleus, and μ is the reduced mass of the system. If we take $m_A \gg m_e$, then $a_0 \approx a_\mu$.

The wavefunctions in 2.6 do not form a complete basis [12], and can therefore be used to compute matrix elements for atomic elements, such as the two-body potential (eqn. 2.4, more in chapter 3).

2.2 Harmonic Oscillator Basis

The hydrogen-like basis functions do not form a complete basis, and in order to ensure that our results converge towards the experimental results this is a necessary condition [13].

Consider the following Hamiltonian:

$$H = \frac{p^2}{2m_e} + V(r). \quad (2.9)$$

Where $V(r)$ is some functional form of a potential. If we wish to find an eigenfunction of this potential, this could be extremely difficult, instead, we shall perform Taylor-Maclaurin expansion.

$$V(r) \approx \frac{1}{0!}V(0) + \frac{r}{1!}\frac{d}{dr}V(0) + \frac{r^2}{2!}\frac{d^2}{dr^2}V(0) + \frac{r^3}{3!}\frac{d^3}{dr^3}V(0) + \dots \quad (2.10)$$

If we consider a very crude assumption that terms beyond some value will be too heavily suppressed to contribute, and that lower order terms contribute too little to meaningfully contribute either then a very rough approximation can be made [9].

$$V(r) \approx \frac{qr^2}{2!}. \quad (2.11)$$

Where q is some parameter that we can vary in order to best approximate the potential. This is the harmonic oscillator potential with a constant $q = \mu\omega^2$.

$$H = \frac{p^2}{2\mu} + \frac{1}{2}\mu\omega^2r^2. \quad (2.12)$$

Where μ is the reduced mass as before, ω is the frequency of a harmonic oscillator. By employing separation of variables, as before, we can show that the solutions to this are as follows:

$$\Psi_{nlm}(r, \theta, \phi) = N_{nl}\tilde{R}_{nl}(r)Y_{lm}(\theta, \phi), \text{ with} \quad (2.13)$$

$$N_{nl} = \sqrt{\sqrt{\frac{2\nu^3}{\pi}} \frac{2^{n+2l+3}n! \nu!}{(2n+2l+1)!!}}, \quad (2.14)$$

$$\tilde{R}_{nl}(r) = r^l e^{-\nu r^2} L_k^{l+\frac{1}{2}}(2\nu r^2), \quad (2.15)$$

$$\nu = \frac{\mu\omega}{2\hbar}. \quad (2.16)$$

Where L are the reduced Laguerre polynomials, Y are the spherical harmonics and N is a normalization term. These wavefunctions form a complete basis and are commonly used in

fields such as nuclear physics [14, 15]. These are not, however, eigenfunctions of the atomic Hamiltonian, and thus the matrix elements for the kinetic and potential terms must be evaluated.

2.2.1 One-body Energy of Harmonic Oscillator

Expanding the kinetic energy terms as ladder operators, it can be shown that the kinetic energy of a harmonic oscillator can be rewritten as:

$$T_{ab} = \langle a|T|b\rangle = \begin{cases} \frac{\hbar\omega}{2}(2n_a + l_a + \frac{3}{2}), & \text{if } n_a = n_b, \\ \frac{\hbar\omega}{2}\sqrt{(n_a)(n_a + l_a + \frac{1}{2})}, & \text{if } n_a = n_b + 1, \\ \frac{\hbar\omega}{2}\sqrt{(n_b)(n_b + l_b + \frac{1}{2})}, & \text{if } n_a = n_b - 1, \\ 0, & \text{otherwise.} \end{cases} \quad (2.17)$$

Where $|a\rangle$ denotes a complete state a with quantum numbers n_a, l_a , etc. The nuclear coulomb potential can then be written as

$$\begin{aligned} V_{ab} = \langle a|V|b\rangle &= Z\hbar c\alpha \int_0^\infty r^2 dr R_{n_a l_a}(r) \frac{1}{r} R_{n_b l_b}(r) \\ &= Z\hbar c\alpha \tilde{R}_{ab}^{(-1)}. \end{aligned} \quad (2.18)$$

Where $\tilde{R}_{ab}^{(\lambda)}$ is the Talmi radial integral given by equation 6.41 in Suhonen, with $\lambda = -1$ [16].

2.3 Laguerre Basis

Consider the Hamiltonian of an atomic system with a nucleus of Z protons as seen in eqn. 2.5. A solution to this Hamiltonian are the Coulomb functions $W(\vec{r})$ eqns 2.19, 2.20, and 2.21.

$$\left(-\nabla^2 - \frac{2Z}{r}\right) W(\vec{r}) = 2E_{nl}W(\vec{r}), \text{ with} \quad (2.19)$$

$$E_{nl} = \frac{-Z^2}{2(n+l+1)^2}, \quad (2.20)$$

$$W_{nlm}(\vec{r}) \propto \left(\frac{2r}{n+l+1} \right)^l L_n^{2l+1} \left(\frac{2r}{n+l+1} \right) e^{\frac{r}{n+l+1}} Y_{lm}(\hat{r}). \quad (2.21)$$

Where L are the associated Laguerre polynomials and Y are the spherical harmonics. These functions do not form a complete basis without the inclusion of the positive energy states in the continuum [17, 18, 19]. Consider the coefficients of r such that they no longer depend on quantum numbers:

$$\frac{n+l+1}{Z} \rightarrow b^{-1}. \quad (2.22)$$

We can rewrite our Hamiltonian in 2.19 as

$$\left(-\nabla^2 - \frac{2\beta_{nl}}{br} \right) \Phi(\vec{r}) = -b^2 \Phi(\vec{r}), \text{ with} \quad (2.23)$$

$$\beta_{nl} = n + l + 1. \quad (2.24)$$

Whose solutions Φ are given by equation 2.25 also known as the Coulomb-Sturmian equations [17].

$$\Phi(\vec{r}) \propto (2rb)^l L_n^{2l+1}(2rb) e^{rb} Y_{lm}(\hat{r}). \quad (2.25)$$

These functions form a complete basis and are orthogonal with respect to the weight function $1/r$; to make them orthogonal with respect to the Euclidean metric d^3r , we will scale $l \rightarrow l + 1/2$ and absorb the weight function into the wavefunctions themselves, yielding the Laguerre functions:

$$\Lambda_{nlm}(\vec{r}) = (2b)^{\frac{3}{2}} \left(\frac{n!}{(n+2l+2)!} \right)^{\frac{1}{2}} (2rb)^l L_n^{2l+2}(2rb) e^{rb} Y_{lm}(\hat{r}). \quad (2.26)$$

These functions are orthogonal on all three quantum numbers, n , l , and m on the usual d^3r metric.

$$\int_0^{4\pi} \int_0^\infty r^2 dr d\Omega \Lambda_{nlm}(\vec{r}) \Lambda_{n'l'm'}(\vec{r}) = \delta_{nn'} \delta_{ll'} \delta_{mm'}. \quad (2.27)$$

We may rewrite Λ in terms of radial and angular components:

$$\Lambda_{nlm} = r^{-1} S_{nl}(r) Y_{lm}(\hat{r}). \quad (2.28)$$

The angular component, S , is only orthogonal in n , however the spherical harmonics ensure orthogonality in l and m . The matrix element of an operator, O , acting on these functions will have the form [17]:

$$\begin{aligned} \langle n'l'm' | O(r, \Omega) | nlm \rangle &= \langle n'l' | O(r) | nl \rangle \langle l'm' | O(\Omega) | lm \rangle \\ \langle n'l' | O(r) | nl \rangle &= \int_0^\infty dr S_{n'l'} r O(r) r^{-1} S_{nl} \\ \int_0^\infty dr S_{n'l'} r O(r) r^{-1} S_{nl} &= \int_0^\infty dr S_{n'l'} \gamma(O(r)) S_{nl} \\ \gamma(O(r)) &= r O(r) r^{-1}. \end{aligned}$$

Note that this definition of b differs slightly from McCoy in that the definition used above is simply the reciprocal of the McCoy's definition [17].

The appeal of the Laguerre basis is that the functions Λ are solutions of a differential equation similar to that of the hydrogen atom. Specifically, the Laguerre basis functions are solutions to the differential equation in 2.29"

$$\left[-\frac{\partial^2}{\partial r^2} - \frac{3}{r} \frac{\partial}{\partial r} + \frac{l(l+2)}{r^2} - 2b \frac{\alpha_{nl}}{r} \right] \Lambda_{nlm} = -b^2 \Lambda_{nlm}. \quad (2.29)$$

Where l is angular momentum and α is defined as:

$$\alpha_{nl} = n + l + \frac{3}{2}. \quad (2.30)$$

By comparison, the differential equation of the hydrogen-like atom is:

$$\left[-\frac{1}{2} \frac{\partial^2}{\partial r^2} - \frac{1}{r} \frac{\partial}{\partial r} + \frac{l(l+1)}{r^2} - \frac{Z}{r} \right] \Phi_{nlm} = -\frac{1}{2} \Phi_{nlm}. \quad (2.31)$$

This is, in fact, the origin of the Laguerre basis, they are derived from the Coulomb-Sturmian basis functions [17] which are solutions to the Sturm-Liouville equation with a Coulomb potential.

2.4 Truncation Parameter

Although a mathematically rigorous treatment of the Hamiltonian would include an infinite number of basis functions, this is computationally impossible to accomplish. Instead, we select a truncation parameter, known as E_{max} , which defines a set of possible wavefunctions that we calculate up to that limit.

In both the harmonic oscillator basis and Laguerre, our truncation parameter is limited by the energy eigenvalues of the eigenfunction from which the basis set is derived. In the harmonic oscillator basis, the energies of the potential are [16]:

$$E_{nl} = \hbar\omega \left(2n + l + \frac{3}{2} \right). \quad (2.32)$$

Thus, we may define a constant E_{max} as the set of all wavefunctions whose quantum numbers $2n + l$ are less than or equal to E_{max} ; where there is an implied unit of energy. For a particle with $1/2$ spin, we can also include all possible j quantum numbers in our basis, where j is defined below.

$$|l - s| \leq j \leq l + s. \quad (2.33)$$

For example, at $E_{max} = 2$, for a spin- $1/2$ particle, the available wavefunctions in the harmonic oscillator basis are:

$$\begin{aligned} E \propto 0 & : |n = 0, l = 0, j = \frac{1}{2}\rangle, \\ E \propto 1 & : |01\frac{1}{2}\rangle, |01\frac{3}{2}\rangle, \\ E \propto 2 & : |10\frac{1}{2}\rangle, |02\frac{3}{2}\rangle, |02\frac{5}{2}\rangle. \end{aligned} \quad (2.34)$$

In the Laguerre basis, the basis functions are eigenfunctions of a potential with a scaling factor shown in equation 2.30. Arbitrarily, it was decided that this definition would serve a reasonable truncation parameter definition. E_{max} in the Laguerre basis is defined by the set of all wavefunctions who quantum numbers $n + l$ are less than or equal to E_{max} . For $E_{max} = 2$:

$$\begin{aligned}
E \propto 0 & : |n = 0, l = 0, j = \frac{1}{2}\rangle, \\
E \propto 1 & : |10\frac{1}{2}\rangle, |01\frac{1}{2}\rangle, |01\frac{3}{2}\rangle, \\
E \propto 2 & : |20\frac{1}{2}\rangle, |11\frac{1}{2}\rangle, |11\frac{3}{2}\rangle, |02\frac{3}{2}\rangle, |02\frac{5}{2}\rangle.
\end{aligned}
\tag{2.35}$$

Chapter 3

Electron-Electron Interaction

One of the key challenges to determining atomic spectra is the interaction between the electrons of an atom. This interaction is difficult not only because of the number of possible calculations required, but also because the basis functions are not eigenfunctions of this interaction, requiring the Hamiltonian to be diagonalized (see Ch. 4).

Derivation of the operators used in sections 3.2 and 3.3 was performed by myself, with advice and assistance from Ragnar Stroberg and Takayuki Miyagi.

3.1 Many-Body Quantum Mechanics

Consider a two-particle system which we assume can be expressed as a product of single-particle wavefunctions, ψ_i , each with its own coordinate space, \vec{x}_i , and we assume each is properly normalized

$$\Psi(\vec{x}_1, \vec{x}_2) \sim \psi_1(\vec{x}_1)\psi_2(\vec{x}_2). \quad (3.1)$$

In order for us to apply this equation for fermions, we must construct a solution which satisfy antisymmetrization under fermion exchange, i.e.:

$$\Psi(\vec{x}_1, \vec{x}_2) = -\Psi(\vec{x}_2, \vec{x}_1). \quad (3.2)$$

Therefore, including antisymmetrization and normalization, we may construct the fol-

lowing wavefunction for our two-particle system eqn. 3.3:

$$\begin{aligned}\Psi(\vec{x}_1, \vec{x}_2) &= \frac{1}{\sqrt{2}} (\psi_1(\vec{x}_1)\psi_2(\vec{x}_2) - \psi_1(\vec{x}_2)\psi_2(\vec{x}_1)) \\ &= \frac{1}{\sqrt{2}} \begin{vmatrix} \psi_1(\vec{x}_1) & \psi_2(\vec{x}_1) \\ \psi_1(\vec{x}_2) & \psi_2(\vec{x}_2) \end{vmatrix}.\end{aligned}\quad (3.3)$$

This is known as a Slater determinant and finding the wavefunctions that satisfy this relation can be exceptionally difficult, even for a simple two-particle system. For a system with N particles, we can construct a much larger Slater determinant:

$$\Psi(\vec{x}_1, \vec{x}_2, \dots, \vec{x}_N) = \frac{1}{\sqrt{N!}} \begin{vmatrix} \psi_1(\vec{x}_1) & \dots & \psi_N(\vec{x}_1) \\ \vdots & \ddots & \vdots \\ \psi_1(\vec{x}_N) & \dots & \psi_N(\vec{x}_N) \end{vmatrix}.\quad (3.4)$$

Instead of putting the burden of anti-symmetrization and normalization, we can assume that our wavefunctions are indeed products of one-body wavefunctions as in equation 3.1. We can then require that the matrix elements themselves are normalized and symmetrized. Consider the following two-body operator O :

$$\begin{aligned}\langle \alpha\beta; J | O | \gamma\delta; J \rangle &= N_{\alpha\beta} N_{\gamma\delta} \sum_{m_\alpha, m_\beta, m_\gamma, m_\delta} \langle \alpha m_\alpha \beta m_\beta | J M_J \rangle \langle \gamma m_\gamma \delta m_\delta | J M_J \rangle \langle \alpha m_\alpha \beta m_\beta | O | \gamma m_\gamma \delta m_\delta \rangle \\ &= N_{\alpha\beta} N_{\gamma\delta} \sum_{m_\alpha, m_\beta, m_\gamma, m_\delta} \langle \alpha m_\alpha \beta m_\beta | J M_J \rangle \langle \gamma m_\gamma \delta m_\delta | J M_J \rangle \\ &\quad \left(\langle \alpha m_\alpha \beta m_\beta | O | \gamma m_\gamma \delta m_\delta \rangle_p - \langle \alpha m_\alpha \beta m_\beta | O | \delta m_\delta \gamma m_\gamma \rangle_p \right).\end{aligned}\quad (3.5)$$

$$|\delta m_\delta \gamma m_\gamma \rangle_p = |\delta m_\delta \rangle |\gamma m_\gamma \rangle\quad (3.6)$$

Where N_{ij} denote normalization constants to be discussed, and the recoupling coefficients, $\langle i m_i j m_j | J M_J \rangle$, denote Clebsch-Gordan coefficients; the brackets with the subscript p denote product of wavefunctions as in equation 3.6. One should also note that the matrix elements on the left hand side of equation 3.5 are independent of angular momentum or spin pro-

jections and that the matrix elements themselves takes into account any effect an operator acting on said projections will have. Using the symmetry properties of the Clebsch-Gordan coefficients [20], we can reduce the sums in equation 3.5 down to

$$\begin{aligned} \langle \alpha\beta; J | O | \gamma\delta; J \rangle &= \frac{1}{\sqrt{(1 + \delta_{\alpha\beta})(1 + \delta_{\gamma\delta})}} \\ &\times \left(\langle \alpha\beta; J | O | \gamma\delta; J \rangle_p - (-1)^{j_\gamma + j_\delta - J} \langle \alpha\beta; J | O | \delta\gamma; J \rangle_p \right). \end{aligned} \quad (3.7)$$

Where the fraction in equation 3.7 satisfies the normalization condition in equation 3.5, and instead we have reduced the operator to two a pair of integrals which is properly normalized and anti-symmetrized. It is worth noting that, if necessary, the terms in equation 3.7 can further be decomposed into projections using Clebsch-Gordan coefficients if necessary.

The reader should assume that all two-body operators stated hereafter are properly normalized and anti-symmetrized for the sake of easier reading.

3.2 Hydrogen-Like and Laguerre Bases

Recall from equation 2.4, the form of our potential.

$$V_{ij} = \frac{\hbar c \alpha}{|\vec{r}_i - \vec{r}_j|},$$

V_{ij} can then be simplified using a multipole expansion to the following:

$$\begin{aligned} V_{ij} &= \frac{\hbar c \alpha}{r_i \sqrt{1 + \frac{r_j^2}{r_i^2} - \frac{r_j}{r_i} \cos \gamma}} \\ V_{ij} &= \hbar c \alpha \sum_l P_l(\cos \gamma) \frac{r_{<}^l}{r_{>}^{l+1}}. \end{aligned} \quad (3.8)$$

Where γ is the angle between the r vectors, P_l is the Legendre polynomial of order l ; taking one of the vectors along the z-axis, then $\gamma \rightarrow \theta_i$. We can couple our matrix elements in the J-scheme to the LS scheme by converting the j coupled kets to summation of LS coupled kets using Wigner 9J symbols [21]. We can then use the spherical harmonics in the wavefunctions and rewrite the integrals of the angular component as Wigner 3J symbols. Putting all of

these changes together, we can write the entire matrix element as

$$\begin{aligned}
&= \langle n_a l_a j_a n_b l_b j_b; J | V_{ij} | n_c l_c j_c n_d l_d j_d; J \rangle \\
&= \sqrt{(2l_a + 1)(2l_b + 1)(2l_c + 1)(2l_d + 1)} \\
&\times \sum_{L_{ab}, S_{ab}, L_{cd}, S_{cd}} \begin{Bmatrix} l_a & s_a & j_a \\ l_b & s_b & j_b \\ L_{ab} & S_{ab} & J \end{Bmatrix} \begin{Bmatrix} l_c & s_c & j_c \\ l_d & s_d & j_d \\ L_{cd} & S_{cd} & J \end{Bmatrix} \\
&\times \sum_{M_{L_{ab}}, M_{S_{ab}}, M_{L_{cd}}, M_{S_{cd}}} \langle L_{ab} M_{L_{ab}} S_{ab} M_{S_{ab}} | J M_{ab} \rangle \langle L_{cd} M_{L_{cd}} S_{cd} M_{S_{cd}} | J M_{cd} \rangle \\
&\times \sum_l \iint R_a R_b \frac{r_{<}^l}{r_{>}^{l+1}} R_c R_d r_1^2 r_2^2 dr_1 dr_2 \begin{pmatrix} l_a & l & l_c \\ 0 & 0 & 0 \end{pmatrix} \begin{pmatrix} l_b & l & l_d \\ 0 & 0 & 0 \end{pmatrix} \\
&\times \sum_{m_{l_a}, m_{l_b}, m_{l_c}, m_{l_d}} \sum_{m=-l}^l (-1)^{m_{l_a} + m_{l_b} + m_{l_c}} \langle l_a m_{l_a} l_b m_{l_b} | L_{ab} M_{L_{ab}} \rangle \langle l_c m_{l_c} l_d m_{l_d} | L_{cd} M_{L_{cd}} \rangle \\
&\times \begin{pmatrix} l_a & l & l_c \\ -m_{l_a} & -m & m_{l_c} \end{pmatrix} \begin{pmatrix} l_b & l & l_d \\ -m_{l_b} & m & m_{l_d} \end{pmatrix}.
\end{aligned} \tag{3.9}$$

Where L_{ab} (and S_{ab}) are all of the possible values that satisfy the triangle condition on l_a, l_b ; $r_{<}$ and $r_{>}$ are the $\min(r_1, r_2)$ and $\max(r_1, r_2)$, respectively. The Wigner 9J symbols come from coupling the wavefunctions in LS as opposed to J-coupled equations [20, 16]. The first set of Clebsch-Gordan coefficients come from coupling all possible projections of total angular momentum and spin to total J projections; the second set of Clebsch-Gordan coefficients come from coupling the individual wavefunction's angular momentum projections to the total angular momentum. The Wigner 3j symbols come from the integral of the spherical harmonic components of the wavefunctions in conjunction with the expansion of the Legendre polynomial in spherical harmonics as follows [16]:

$$P_l(\cos\gamma) = \frac{4\pi}{2l+1} \sum_{m=-l}^l Y_{lm}(\Omega_1) Y_{lm}^*(\Omega_2). \tag{3.10}$$

Where γ is the angle between Ω_1 and Ω_2 , and P_l is simply the Legendre polynomial, and the \star indicates the complex conjugate. Substituting this into eqn 3.8 and omitting the radial

component gives:

$$\begin{aligned}
& \frac{4\pi}{2l+1} \sum_{m=-l}^l \int \int d\Omega_1 d\Omega_2 Y_a^*(\Omega_1) Y_b^*(\Omega_2) Y_{lm}(\Omega_1) Y_{lm}^*(\Omega_2) Y_c(\Omega_1) Y_d(\Omega_2) \\
&= \sqrt{(2l_a+1)(2l_b+1)(2l_c+1)(2l_d+1)} \begin{pmatrix} l_a & l & l_c \\ 0 & 0 & 0 \end{pmatrix} \begin{pmatrix} l_b & l & l_d \\ 0 & 0 & 0 \end{pmatrix} \\
&\times \begin{pmatrix} l_a & l & l_c \\ -m_{l_a} & -m & m_{l_c} \end{pmatrix} \begin{pmatrix} l_b & l & l_d \\ -m_{l_b} & m & m_{l_d} \end{pmatrix}.
\end{aligned} \tag{3.11}$$

Where a, b , etc. represent all of the relevant quantum numbers for the states a, b etc. The second line in eqn. 3.11, relies on the following identity [16]:

$$\begin{aligned}
& \int d\Omega Y_{l_a m_a}(\Omega) Y_{l_b m_b}(\Omega) Y_{l_c m_c}(\Omega) \\
&= \sqrt{\frac{(2l_a+1)(2l_b+1)(2l_c+1)}{4\pi}} \begin{pmatrix} l_a & l_b & l_c \\ 0 & 0 & 0 \end{pmatrix} \begin{pmatrix} l_a & l_b & l_c \\ m_a & m_b & m_c \end{pmatrix}.
\end{aligned} \tag{3.12}$$

Although this operator is mathematically correct, it is computationally intense due to the large number of terms required to calculate. Instead, we can evaluate matrix elements in the jj -coupling scheme and avoid having to recouple our matrix elements.

Starting with equation 3.10, and using the Wigner-Eckart Theorem [22], we can rewrite 3.10 as a product of spherical tensors:

$$P_l(\cos\gamma) = \frac{4\pi}{2l+1} T^l(\Omega_1) \cdot T^l(\Omega_2). \tag{3.13}$$

The angular component of the integral can be expressed as

$$\begin{aligned}
& \langle l_1 j_1 l_2 j_2; JM_J | T^l(\Omega_1) \cdot T^l(\Omega_2) | l_3 j_3 l_4 j_4; JM_J \rangle, \\
&= (-1)^{j_2+J+j_3} \begin{Bmatrix} j_1 & j_2 & J \\ j_4 & j_3 & l \end{Bmatrix} \langle l_1 j_1 | T^l(\Omega_1) | l_3 j_3 \rangle \langle l_2 j_2 | T^l(\Omega_2) | l_4 j_4 \rangle.
\end{aligned} \tag{3.14}$$

The onebody angular components can then be simplified further to

$$\begin{aligned}
& \langle \frac{1}{2}l_1j_1 | T^l(\Omega_1) | \frac{1}{2}l_3j_3 \rangle = \\
& (-1)^{j_1 - \frac{1}{2}} \sqrt{\frac{(2j_1 + 1)(2l + 1)(2j_3 + 1)}{4\pi}} \begin{pmatrix} j_1 & l & j_3 \\ -\frac{1}{2} & 0 & \frac{1}{2} \end{pmatrix} \frac{1}{2} (1 + (-1)^{j_1 + j_3 + l}). \quad (3.15)
\end{aligned}$$

We can use the limited range of non-zero values in the 3J symbol to limit which values l are allowable. We also know that the last bracket in the equation is either 0 or 2, so we can iterate over only the non-zero terms. Combining the results of equations 3.13, and 3.15, we can write our matrix elements as

$$\begin{aligned}
& \langle n_a l_a j_a n_b l_b j_b; J | V_{ij} | n_c l_c j_c n_d l_d j_d; J \rangle, \\
& = (-1)^{j_1 + j_3 + J} \hat{j}_1 \hat{j}_2 \hat{j}_3 \hat{j}_4 \sum_{l=\hat{l}_{min}}^{\hat{l}_{max}} I_{n_a l_a j_a n_b l_b j_b n_c l_c j_c n_d l_d j_d}^l \begin{Bmatrix} j_1 & j_2 & J \\ j_4 & j_3 & l \end{Bmatrix} \begin{pmatrix} j_1 & l & j_3 \\ -\frac{1}{2} & 0 & \frac{1}{2} \end{pmatrix} \begin{pmatrix} j_2 & l & j_4 \\ -\frac{1}{2} & 0 & \frac{1}{2} \end{pmatrix}. \quad (3.16)
\end{aligned}$$

Where \hat{j}_i is the usual hat notation used in nuclear physics:

$$\hat{j}_i = \sqrt{2j_i + 1}. \quad (3.17)$$

Note that in equation 3.16, the equation is 0 unless the following conditions are true:

$$\text{mod}(l_1 + l + l_3, 2) = 0,$$

$$\text{mod}(l_2 + l + l_4, 2) = 0.$$

Where I is the integral over the radial component of the operator:

$$I_{n_a l_a j_a n_b l_b j_b n_c l_c j_c n_d l_d j_d}^l = \int_0^\infty \int_0^\infty r_1^2 r_2^2 dr_1 dr_2 R_{n_a l_a}(r_1) R_{n_b l_b}(r_2) R_{n_c l_c}(r_1) R_{n_d l_d}(r_2) \frac{r_1^{l_<}}{r_1^{l_>}}. \quad (3.18)$$

This integral is solved numerically using an adaptive numerical integration library, ‘‘Cubature’’ [23]. Once this equation is solved for a particular value of b , a change of variables can be performed to scale the value of the integral for any value of b :

$$\begin{aligned}
r &= \frac{r'}{b}, \\
br &= r', \\
\frac{(br)_{<}^l}{(br)_{>}^{l+1}} &= b \frac{r_{<}^l}{r_{>}^{l+1}}.
\end{aligned} \tag{3.19}$$

Thus after a change of variables, we can solve for any value of b by scaling the solution at $b = 1$ by a factor of b :

$$I_{n_a l_a j_a n_b l_b j_b n_c l_c j_c n_d l_d j_d}^l(b) = b I_{n_a l_a j_a n_b l_b j_b n_c l_c j_c n_d l_d j_d}^l(b = 1). \tag{3.20}$$

This, of course, assumes that the value of b is the same for all wavefunctions. If different wavefunctions had different values of b a more sophisticated approach would be required. Caprio, Maris, and Vary proved that the Coulomb-Sturmian basis can still form a complete basis for multiple values of b provided that there exists a unique value of b for each unique value of l [24].

3.3 Harmonic Oscillator Basis

Consider a two-particle system in a harmonic oscillator potential. The general form of the Hamiltonian is:

$$H = H_1 + H_2 = \frac{p_1^2}{2m_1} + \frac{1}{2}m\omega r_1^2 + \frac{p_2^2}{2m_2} + \frac{1}{2}m\omega r_2^2. \tag{3.21}$$

Where p_i , m_i , r_i are the position, mass, and position of the i th particle, respectively. We can then express a total and reduced mass, as well as centre-of-mass and relative positions as follows

$$\mu = \left(\frac{1}{m_1} + \frac{1}{m_2} \right)^{-1}, \tag{3.22}$$

$$M = m_1 + m_2, \tag{3.23}$$

$$R = r_1 + r_2, \tag{3.24}$$

$$r = \frac{|r_1 - r_2|}{2}. \quad (3.25)$$

Rearranging the Hamiltonian in 3.21, we can rewrite it in terms of relative (*rel*) and centre-of-mass (*CM*) coordinates.

$$H = H_{CM} + H_{rel} = \frac{P^2}{2M} + \frac{1}{2}M\omega R^2 + \frac{p^2}{2\mu} + \frac{1}{2}\mu\omega r^2. \quad (3.26)$$

Where P is the momentum operator in the centre-of-mass frame, and p is the momentum operator in the relative frame. We may then rewrite our basis functions in terms of relative and centre-of-mass quantum numbers.

$$|(n_1 l_1) (n_2 l_2) L\rangle = \sum_{n\lambda N\Lambda} \langle n\lambda N\Lambda L | n_1 l_1 n_2 l_2 L \rangle |(n\lambda) (N\Lambda) L\rangle. \quad (3.27)$$

Where N and Λ are centre-of-mass quantum numbers, and n and λ are relative quantum numbers, and the summation is over all possible quantum numbers that conserve energy and angular momentum. This is referred to as a Talmi-Moshinsky transformation [16, 25], and it allows us to reduce complicated two-body matrix elements in one reference frame into a summation of one-body matrix elements in a different frame. Take, for example, the electron-electron interaction given by equation 2.4:

$$V_{ab} = \frac{\hbar c \alpha}{|\vec{r}_a - \vec{r}_b|} = \frac{\hbar c \alpha}{r}.$$

The matrix elements of this potential as follows:

$$\begin{aligned}
& \langle (n_a l_a) (n_b l_b) J_{ab} | |V_{ab}| | (n_c l_c) (n_d l_d) J_{cd} \rangle \\
&= \sum_{n\lambda N\Lambda, n'\lambda' N'\Lambda'} \langle n\lambda N\Lambda J_{ab} | n_a l_a n_b l_b; J_{ab} \rangle \langle n'\lambda' N'\Lambda' J_{cd} | n_c l_c n_d l_d; J_{cd} \rangle \\
&\times \langle (n\lambda) (N\Lambda); J_{ab} | \left| \frac{\hbar c \alpha}{r} \right| | (n'\lambda') (N'\Lambda'); J_{cd} \rangle \\
&= \sum_{n\lambda N\Lambda, n'\lambda' N'\Lambda'} \langle n\lambda N\Lambda; J_{ab} | n_a l_a n_b l_b; J_{ab} \rangle \langle n'\lambda' N'\Lambda'; J_{cd} | n_c l_c n_d l_d; J_{cd} \rangle \\
&\times \langle n\lambda | \left| \frac{\hbar c \alpha}{r} \right| | n'\lambda' \rangle \delta_{NN'} \delta_{\Lambda\Lambda'} \\
&= \sum_{n\lambda N\Lambda, n'\lambda' N'\Lambda'} \langle n\lambda N\Lambda J_{ab} | n_a l_a n_b l_b; J_{ab} \rangle \langle n'\lambda' N'\Lambda' J_{cd} | n_c l_c n_d l_d; J_{cd} \rangle \\
&\times \left\{ \begin{array}{ccc} \lambda & \lambda & 0 \\ J_{ab} & J_{cd} & \Lambda \end{array} \right\} \hbar c \alpha \tilde{R}_{n\lambda, n'\lambda'}^{(-1)} \sqrt{(2J_{ab} + 1)(2J_{cd} + 1)(2\lambda + 1)} \delta_{NN'} \delta_{\Lambda\Lambda'} \delta_{\lambda\lambda'}.
\end{aligned} \tag{3.28}$$

In the final step in equation 3.28, we were able to reduce the two-body interaction down to a one-body interaction with a similar form to equation 2.18. Despite the fact that there are many coefficients and integrals to solve, many of them are repeated between different matrix elements, and can be pre-calculated and cached, saving a great deal of computational effort.

Similar to the Laguerre basis, we can solve the harmonic oscillator for $\hbar\omega = 1$ and perform a change of variables and we find that our scaling factor is $\sqrt{\hbar\omega}$:

$$V_{ab}(\hbar\omega) = \sqrt{\hbar\omega} V_{ab}(\hbar\omega = 1). \tag{3.29}$$

The ability to perform these change of variables means that we are able to calculate our matrix elements once and save them to disk and all subsequent calculations can simply be read from file and scaled, saving enormous computational effort.

Chapter 4

IM-SRG

In this thesis, the main purpose is to solve the many-body Schrödinger equation and in doing so, determine the eigenfunctions of the atomic Hamiltonian. In this section, we will first discuss the Hartee-Fock method (see e.g. [26]), and the limitations thereof.

4.1 Hartree-Fock Method

Consider a wavefunction in state $|C\rangle$, we may determine the expectation value of the energy using the Hamiltonian (eqn 4.1, we are assuming that the state $|C\rangle$ is an eigenfunction of the Hamiltonian) [20].

$$\begin{aligned} E_C &= \langle C | H | C \rangle = \langle H \rangle \\ &= \sum_n \langle n | H^{(1)} | n \rangle + \sum_{n,m} \langle nm | H^{(2)} | nm \rangle. \end{aligned} \tag{4.1}$$

Where $H^{(1)}$ denotes the one-body component of the Hamiltonian and $H^{(2)}$ denotes the two-body component. Similarly, the energy of state $|C + k\rangle$, which is the same as state $|C\rangle$, but with an additional particle in state k above the Fermi level, is E_{C+k} . The difference between these energies can be defined as δE_{C+k} .

$$E_{C+k} = \langle C + k | H | C + k \rangle = E_C + \langle k | H^{(1)} | k \rangle + \sum_n \langle nk | H^{(2)} | nk \rangle, \tag{4.2}$$

$$\delta E_{C+k} = E_{C+k} - E_C = \langle k | H^{(1)} | k \rangle + \sum_n \langle nk | H^{(2)} | nk \rangle. \quad (4.3)$$

One can also derive similar functions for the addition of two particles above the Fermi level, or removing of particles below the Fermi level as well as the differences between these energies, but essentially, these will have forms similar to equations 4.1-4.3.

4.1.1 Variational Principle

Consider some normalized wavefunction, with some undetermined parameter, b i.e. $\Psi(\vec{r}, b)$. The variational principle states that for any normalized wavefunction, we can determine some upper bound on the ground state energy of the system described by some Hamiltonian [9].

$$E_g \leq \langle \Psi(\vec{r}, b) | H | \Psi(\vec{r}, b) \rangle = \langle H \rangle. \quad (4.4)$$

We can set a best fit for the parameter b by minimizing $\langle H \rangle$ with respect to b (eqn. 4.5).

$$\frac{\partial}{\partial b} \langle H \rangle = 0. \quad (4.5)$$

4.1.2 Hartree-Fock Method

In a Hartree-Fock method [9], we exploit the variational principle (sec. 4.1.1) in an attempt to minimize the energy E_C with respect to small changes in our basis functions, $\phi_i(\vec{r})$ (or $\phi_i^*(\vec{r})$) [20]

$$\frac{\partial}{\partial \phi_i(\vec{r})} \left(E_C + \sum_a \lambda_a \int |\phi_a(\vec{r})|^2 d\vec{r} \right) = 0. \quad (4.6)$$

Where λ_a are as yet undetermined Lagrange multipliers which enforce normalization. It can be shown (see e.g., [20]) that these Lagrange multipliers are actually the energy differences:

$$\lambda_a = \delta E_{C+a} = E_{C+a} - E_C = \langle a | H^{(1)} | a \rangle + \sum_n \langle na | H^{(2)} | na \rangle. \quad (4.7)$$

We can consider the final term in eqn. 4.7, to be some expectation value for a mean field.

$$\sum_n \langle na | H^{(2)} | na \rangle = \langle a | U^{HF} | a \rangle. \quad (4.8)$$

We may then rewrite the Hamiltonian in the Hartree-Fock basis as follows

$$H = H^{(0)} + W, \quad (4.9)$$

$$H^{(0)} = \sum_k \left(H_k^{(1)} + U_k^{HF} \right), \quad (4.10)$$

$$W = \sum_{kl} H_{kl}^{(2)} - \sum_k U_k^{HF}. \quad (4.11)$$

The energy of a particle in this state ($|C\rangle = |\Phi_{HF}\rangle$) is simply the sum of the so-called zeroth and first order Hartree-Fock energies,

$$E_{HF}^{(0)} = \langle \Phi_{HF} | \sum_k \left(H_k^{(1)} + U_k^{HF} \right) | \Phi_{HF} \rangle = \sum_\alpha \lambda_\alpha, \quad (4.12)$$

$$\begin{aligned} E_{HF}^{(1)} &= \langle \Phi_{HF} | W | \Phi_{HF} \rangle \\ E_{HF}^{(1)} &= -\frac{1}{2} \sum_{n,m} \langle nm | H^{(2)} | nm \rangle. \end{aligned} \quad (4.13)$$

Where λ_α is the same as in eqn. 4.7. By solving the Hartree-Fock energies, we can create a set of basis functions which form a better basis set than our original wave functions (see e.g. [1, 3]).

4.1.3 Limitations of the Hartree-Fock Method

While the Hartree-Fock method has shown to be extremely accurate, it often fails to account for all of the physics of a many-body system. For example, the Hartree-Fock method fails to account for the correlation between electrons [27]. Despite its limitations, however, it does provide fairly accurate predictions for ground state wavefunctions, as well as forming an excellent basis, $|\Phi_{HF}\rangle$, which will be used by the In-Medium Similarity Normalization Group method.

4.2 In-Medium Similarity Normalization Group

Similarity Renormalization Group (SRG) was first developed by several sources including Wegner for the purpose of evaluating Hamiltonians in condensed matter systems [28]. The principle behind this operation is the transformation of the Hamiltonian by a unitary operator subject to some flow parameter, s

$$\tilde{H}(s) = U(s)H(0)U^\dagger(s) = \tilde{H}^d(s) + \tilde{H}^{od}(s), \text{ with} \quad (4.14)$$

$$\lim_{s \rightarrow \infty} \tilde{H}^{od}(s) = 0. \quad (4.15)$$

Where $H(s = 0)$ is simply the initial, untransformed Hamiltonian, $\tilde{H}^d(s)$ is the diagonal portion of the Hamiltonian, and $\tilde{H}^{od}(s)$ is the off-diagonal portion. In general, $U(s)$ can take many forms depending on the application, and whether or not the aim is to block-diagonalize, i.e. ,fully diagonalize the Hamiltonian [4]. We can determine the form of U by differentiating \tilde{H} with respect to s

$$\begin{aligned} \frac{d\tilde{H}(s)}{ds} &= \frac{dU(s)}{ds} \tilde{H}(0)U^\dagger(s) - U(s) \tilde{H}(0) \frac{dU^\dagger(s)}{ds} \\ \frac{d\tilde{H}(s)}{ds} &= \frac{dU(s)}{ds} U^\dagger(s) \tilde{H}(s) - \tilde{H}(s) U(s) \frac{dU^\dagger(s)}{ds} \end{aligned} \quad (4.16)$$

$$\frac{d\tilde{H}(s)}{ds} = [\eta(s), \tilde{H}(s)] \quad (4.17)$$

$$\eta(s) = \frac{dU(s)}{ds} U^\dagger(s) = -\eta^\dagger(s). \quad (4.18)$$

Given that the U matrix is required to be unitary, we can rearrange equation 4.18 to a familiar format.

$$\begin{aligned} \eta(s) &= \frac{dU(s)}{ds} U^\dagger(s), \\ \eta(s)U(s) &= \frac{dU(s)}{ds} U^\dagger(s)U(s), \end{aligned} \quad (4.19)$$

$$\eta(s)U(s) = \frac{dU(s)}{ds}, \text{ with}$$

$$U(s) = Ae^{\int_0^s \eta(s') ds'}. \quad (4.20)$$

As mentioned in the paragraph above, the exact form of η depends on what the user seeks to accomplish. In practice, the transformation is not a one-off operation, but rather a series of infinitesimal operations

$$U(s) = \lim_{N \rightarrow \infty} \prod_{i=0}^N e^{\eta(s_i)\delta s_i}. \quad (4.21)$$

Where we define s_i and δs_i as follows:

$$\begin{aligned} s_{i+1} &= s_i + \delta s_i, \text{ with} \\ \sum_i s_i &= s. \end{aligned} \quad (4.22)$$

Wegner noted that for the operation to cease at some appropriately transformed Hamiltonian, the following relation is a reasonable condition on η [28].

$$\eta(s) \equiv [H^d(s), H(s)]. \quad (4.23)$$

Equation 4.23 will go to zero under two conditions: that the diagonal portion of the Hamiltonian is degenerate with the off-diagonal portion of the Hamiltonian, or if the off-diagonal portion goes to zero [28, 29]. In figure 4.1, one can see a small demonstration of how the Hamiltonian matrix evolves as a function of the flow parameter. The p and h notations refer to excitations above the reference state, for example $1p1h$ refers to the states with 1 particle 1 hole excitation; white squares indicate zero-valued matrix elements, coloured squares are non-zero.

Figure 4.1 is a rough illustration of how the matrix is initially non-zero (or mostly non-zero), and as the flow parameter is evolved, matrix elements may be changed somewhat (indicated by the colour changes). The elements which indicate an overlap of the excitations and the ground state, however, go to zero, illustrated by those states going white.

4.3 Normal-Ordering and Wick's Theorem

Consider usual creation and annihilation operators for a fermionic system have the following anti-commutation relations:

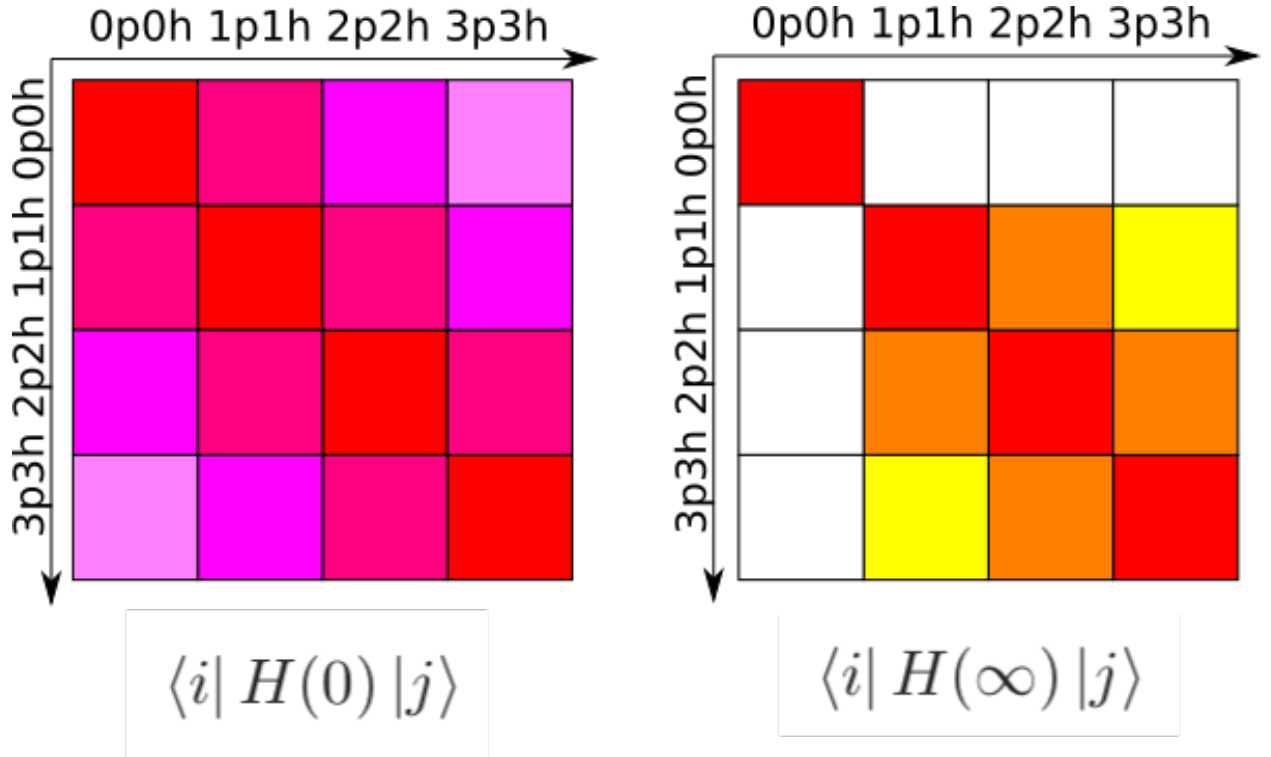


Figure 4.1: Evolution of the Hamiltonian matrix with respect to the flow parameter.

$$\begin{aligned}
 \{a_i^\dagger, a_j^\dagger\} &= 0, \\
 \{a_i, a_j\} &= 0, \\
 \{a_i^\dagger, a_j\} &= \delta_{ij}.
 \end{aligned}
 \tag{4.24}$$

Where a_i^\dagger and a_i denote the usual creation and annihilation operators, respectively, for a state with a full set of quantum numbers described by the subscripts i and j . We may describe a Slater determinant for an A -particle system as follows:

$$|\Phi \{i_1, i_2, \dots, i_A\}\rangle = \prod_{k=1}^A a_{i_k}^\dagger |0\rangle.
 \tag{4.25}$$

Where $|0\rangle$ denotes a reference, the vacuum state. The “In-Medium” portion of IM-SRG comes from the fact that we do not use the vacuum as our reference, but instead we have some basis state $|\Phi_0\rangle$, which we generate from a Hartree-Fock method (see section 4.1). Thus, wavefunction is actually

$$|\Phi\{i_1, i_2, \dots, i_A\}\rangle = \prod_{k=1}^A a_{i_k}^\dagger |\Phi_0\rangle. \quad (4.26)$$

We may then define operators using normal ordering as excitations of particles and holes above our reference state.

$$a_i^\dagger a_j \equiv: a_i^\dagger a_j : + \overline{a_i^\dagger a_j}. \quad (4.27)$$

Where the third term is can simply be defined as the expectation value of the operator with respect to our reference state $|\Phi_0\rangle$

$$\overline{a_i^\dagger a_j} \equiv \langle \Phi_0 | a_i^\dagger a_j | \Phi_0 \rangle \equiv \rho_{ij}. \quad (4.28)$$

More generally, for an atom with Z particles, we can generalize equation 4.27 as follows:

$$\begin{aligned} & a_{i_1}^\dagger \dots a_{i_Z}^\dagger a_{j_Z} \dots a_{j_1} \\ & \equiv: a_{i_1}^\dagger \dots a_{i_Z}^\dagger a_{j_Z} \dots a_{j_1} : \\ & + \overline{a_{i_1}^\dagger a_{j_1}} : a_{i_2}^\dagger \dots a_{i_Z}^\dagger a_{j_Z} \dots a_{j_2} : - \overline{a_{i_1}^\dagger a_{j_2}} : a_{i_2}^\dagger \dots a_{i_Z}^\dagger a_{j_Z} \dots a_{j_3} a_{j_1} : + \textit{singles} \\ & + (\overline{a_{i_1}^\dagger a_{j_1} a_{i_2}^\dagger a_{j_2}} - \overline{a_{i_1}^\dagger a_{j_2} a_{i_2}^\dagger a_{j_1}}) : a_{i_3}^\dagger \dots a_{i_Z}^\dagger a_{j_Z} \dots a_{j_3} : + \textit{doubles} \\ & + \dots \end{aligned} \quad (4.29)$$

Where *singles* and *doubles* refer to the number of contractions, which continue until all possible contractions are made [1]. We may then define our Hamiltonian in terms of normal ordered operators [1, 4, 5]

$$H = T + V + V^{(2)}. \quad (4.30)$$

Where T is the kinetic energy, V is the Coulomb potential from the nucleus, and $V^{(2)}$ is the electron-electron Coulomb interaction:

$$H = E + \frac{1}{(2!)^2} \sum_{i,j} f_{ij} : a_i^\dagger a_j : + \frac{1}{(3!)^2} \sum_{ijkl} \Gamma_{ijkl} : a_i^\dagger a_j^\dagger a_k a_l :, \quad (4.31)$$

$$E = \sum_a \langle a | T + V | a \rangle n_a + \frac{1}{2!} \sum_{a,b} \langle ab | V^{(2)} | ab \rangle n_a n_b, \quad (4.32)$$

$$f_{ij} = \langle i | T + V | j \rangle + \sum_a \langle ia | V^{(2)} | ja \rangle n_a, \quad (4.33)$$

$$\Gamma_{ijkl} = \langle ij | V^{(2)} | kl \rangle. \quad (4.34)$$

By working in the one-body density, we can limit the terms over the occupied sums alone [1]. For a much more in depth discussion in the context of nuclear many-body calculations, see [1] or [3].

Taking equation 4.17 and applying Wick's Theorem [30], we are able to construct equations 4.32, 4.33 and 4.34 as they relate to the flow parameter, s [4, 31, 32]

$$\frac{dE}{ds} = \sum_{ij} (n_i - n_j) \eta_{ij} f_{ij} + \frac{1}{2} \sum_{ijkl} \eta_{ijkl} \Gamma_{kl ij} n_i n_j \bar{n}_k \bar{n}_l, \quad (4.35)$$

$$\begin{aligned} \frac{df_{ij}}{ds} &= \sum_a (1 + P_{ia}) \eta_{ia} f_{aj} + \sum_{ab} (n_a - n_b) (\eta_{ab} \Gamma_{biaj} - f_{ab} \eta_{biaj}), \\ &+ \frac{1}{2} \sum_{abc} (n_a n_b \bar{n}_c + \bar{n}_a \bar{n}_b n_c) P_{ij} \eta_{ciab} \Gamma_{abcj}, \end{aligned} \quad (4.36)$$

$$\begin{aligned} \frac{d\Gamma_{ijkl}}{ds} &= \sum_a ((1 - P_{ij})(\eta_{ia} \Gamma_{ajkl} - f_{ia} \eta_{ajkl}) - (1 - P_{kl})(\eta_{ak} \Gamma_{ijal} - f_{ak} \eta_{ijal})) \\ &+ \frac{1}{2} \sum_{ab} (1 - n_a - n_b) (\eta_{ijab} \Gamma_{abkl} - \Gamma_{ijab} \eta_{abkl}) \\ &- \sum_a b(n_a - n_b) (1 - P_{ij})(1 - P_{kl}) \eta_{bjal} \Gamma_{aibk}. \end{aligned} \quad (4.37)$$

Where P_{ij} is the operator which exchanges indices i and j , n_a is the one-body density of the a^{th} orbit and $\bar{n}_a = 1 - n_a$. These flow equations allow us to evolve our Hamiltonian with respect to the flow parameter and block-diagonalize our matrix.

Chapter 5

Extrapolation methods

One of the challenges faced in many-body physics is the poor convergence of basis sets when trying to solve the many-body Schrödinger equation, where convergence denotes how results of one calculation and a relatively low E_{max} differs with that of a calculation at higher E_{max} . A calculation is considered converged when the difference between two calculations at different E_{max} is zero (or very small).

If our basis functions are unable to adequately represent our function on a scale that is computationally feasible, we must often resort to extrapolation effort in order to estimate the value at some limit, and many methods exist [33]

5.1 Least Squares

Consider a set of data points, y , which we attempt to model as some function, $f(x, \theta)$, for some set of inputs, x , and a set of configurable parameters, θ . If the function f reasonably approximates y for all x , then we can say [34]:

$$\begin{aligned}y &\approx f(x, \theta), \\0 &\approx f(x, \theta) - y, \\0 &\leq (f(x, \theta) - y)^2.\end{aligned}\tag{5.1}$$

In the final line of eqn. 5.1, we can see that this function will be at a minima when the values of θ are such that f most closely matches y . This is known as least square fitting,

and is widely used to fit a function to some set of data points [34]. This method can be extremely powerful, and can result in excellent fitting of a curve, provided that the choice of function is already a reasonable approximation to the data. A strong caveat with this method is that a curve with more degrees of freedom (a larger set of values in θ , known as degrees of freedom) will almost always fit closer to data than one with fewer parameters, but that does not necessarily mean that it is actually a better representative of the data.

5.2 Exponential Fitting functions

One of the limitations of many-body physics is the size of the Hamiltonian matrix which we are trying to solve. We truncate the size of our matrix by limiting the set of allowed wavefunctions, and by solving at larger and larger truncation we will attempt to extrapolate the results for an infinitely large Hamiltonian matrix. For small truncation, our Hamiltonian is sensitive to changes in the parameters of our wavefunctions, such as the energy of the quantum harmonic oscillator, $\hbar\omega$, or the length parameter in our Coulomb-Sturmian function, b ; however at infinitely large Hamiltonian matrix will be independent of these parameters [33, 35].

When we calculate some property of our many-body system (such as the ground state energy), we get some estimate of this parameter up to the truncation parameter, E_{max} , we seek an extrapolation such that as $E_{max} \rightarrow \infty$, for our result to yield some sensible limit [33].

As a concrete example, let us consider a series of calculations of the ground-state energy of helium in the Harmonic oscillator basis, each performed at $\hbar\omega = 100\text{eV}$ from $E_{max} = 4$ to $E_{max} = 24$ in increments of 4. Naïvely, the datapoints appear to follow approximately an exponential decay, so we will attempt to fit the following function:

$$E_{GroundState}(E_{max}) = Ne^{-kE_{max}} + E_{\infty}. \quad (5.2)$$

Where N , E_{∞} , and k are the parameters of the exponential which we are trying to fit. Looking at figure 5.1, we can see that the extrapolated value of the function is approximately -77.17 eV, using Hartree-Fock, the limit of which should be -77.87 eV [10].

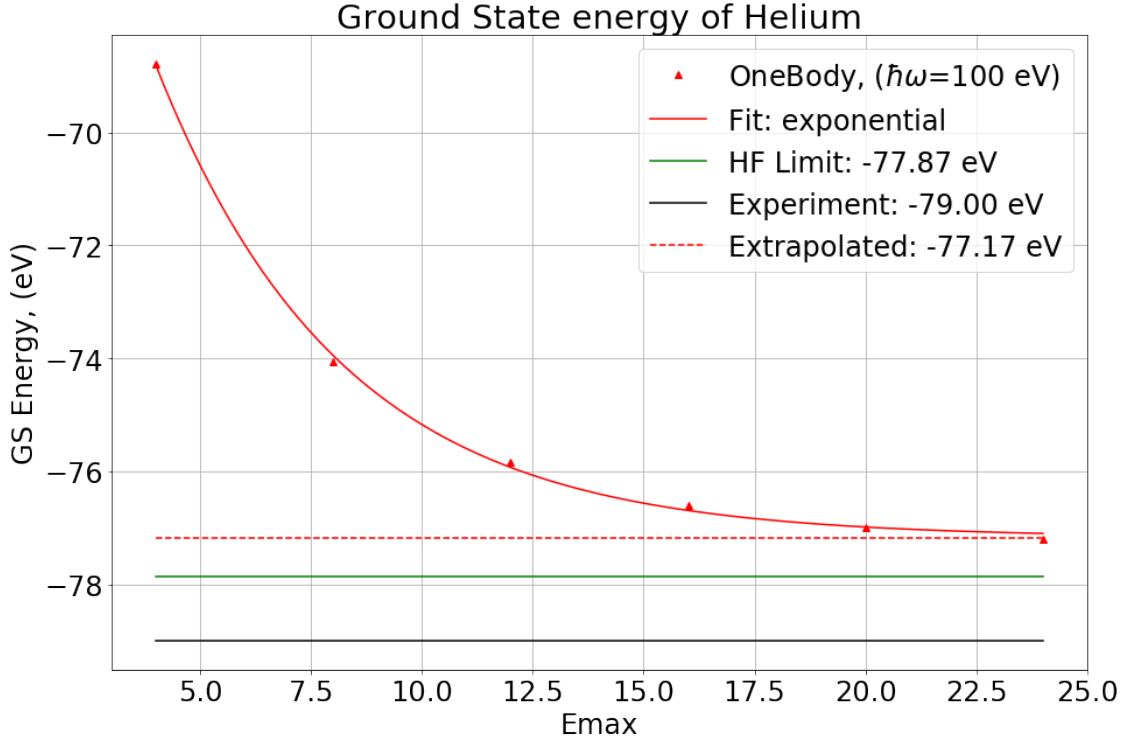


Figure 5.1: Extrapolation of the ground state energy of helium as a function of the truncation parameter, E_{max} , using an exponential fit.

Figure 5.1 shows how the calculated value of the Hartree-Fock energy as a function of the truncation parameter, E_{max} for a particular value of $\hbar\omega$. The experimental value for helium and all other atomic elements is from the National Institute of Standards and Technology (NIST) Atomic Spectra Database [36] in the USA. It should be noted that the experimental value is known to an exceptional level of precision and its uncertainty is incredibly small. The ground state energy of helium, for example, is $-79.0051538 \text{ eV} \pm 0.0000005 \text{ eV}$ [36].

Upon close examination of figure 5.1, we can see that the point at $E_{max} = 24$ actually falls below the extrapolated value of the exponential. If we wish to reduce our difference between the fit and the data, we may instead try a new fitting function. In an effort to try to determine a better fit, we will try a new trial fitting function, a Gaussian (eqn. 5.3):

$$E_{GroundState}(E_{max}) = Ne^{-(k_2 E_{max}^2 + k_1 E_{max})} + E_{\infty}. \quad (5.3)$$

This function is similar to the exponential in equation 5.2, but has an additional degree of freedom by fitting an extra E_{max}^2 term in the exponential.

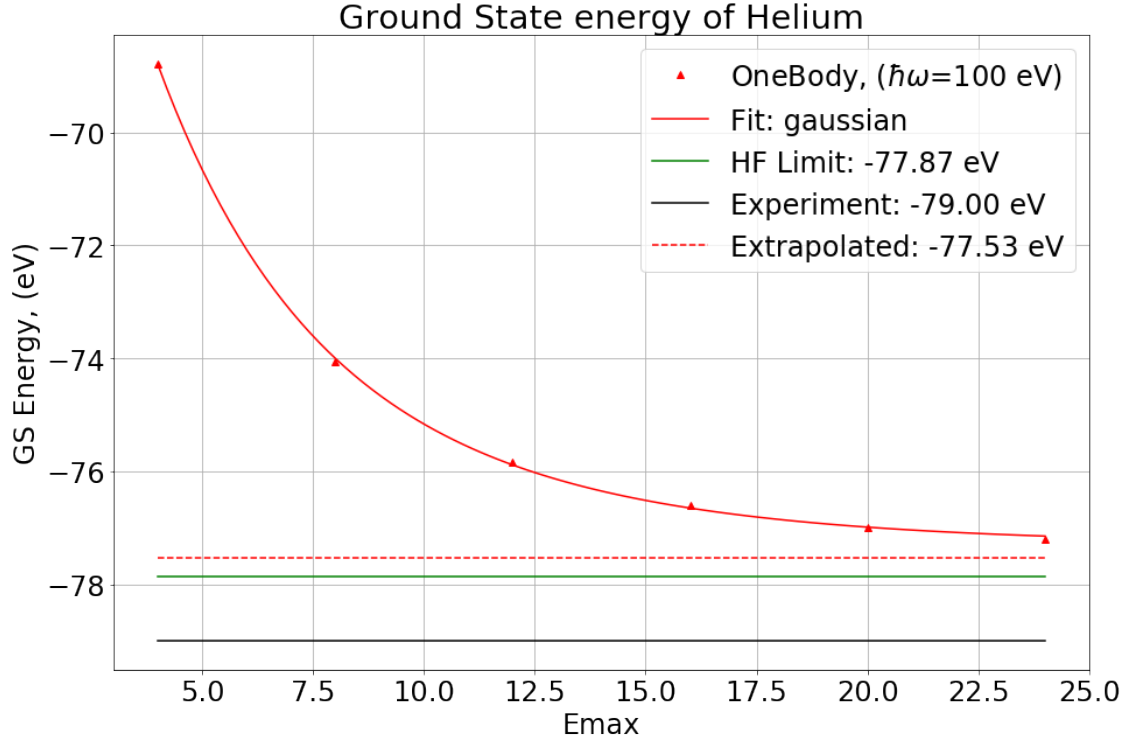


Figure 5.2: Extrapolation of the ground state energy of helium as a function of the truncation parameter, E_{max} , using a Gaussian fit.

Looking at figure 5.2, we can see that this fit is extremely close to the previous fit except that it does not grossly overestimate the final point at $E_{max} = 24$. Taking the mean absolute error, we can see that the mean absolute error is approximately 0.04 eV, thus it is an improvement over the exponential fitting. Many other extrapolation methods exist [35], including machine learning [37, 38] but for the sake of brevity, exponential and Gaussian extrapolations will be used.

Chapter 6

Calculation Method

This section discussed in more detail how the methods presented are put into practice, including how matrix elements are calculated and stored. In both the harmonic oscillator and Laguerre bases, the matrix elements are pre-calculated and saved to disk for long-term use, although the file format and a few minor details are different. The basic method follows this order:

1. Setup orbits and initialize memory space.
2. Calculate one-body matrix elements.
3. Load two-body matrix elements from file and scale.
4. Solve the Hartree-Fock Method.
5. Evolve the Hamiltonian using the IM-SRG.
6. Return files and save results to disk.

Setting up the memory space and calculating the one-body components of the Hamiltonian are fundamentally almost identical for both bases, only the form of the operators and the meaning of the basis functions differs. The two-body components, discussed in sections 6.1 and 6.2, are similar in principle but differ in how the matrix elements are stored.

Once the matrix elements of the Hamiltonian have been calculated and loaded into memory for the given set of basis functions, the rest of the calculation is agnostic of the underlying

basis functions. The Hartree-Fock method from section 4.1.2 and a new set of basis functions is constructed in the Hartree-Fock basis. The Hamiltonian in this basis is then evolved using the IM-SRG method as described in section 4.2. Once the norm of the η matrix reaches a lower limit (less than 10^{-8}), the IM-SRG calculation halts. Any operators which are not part of the Hamiltonian are then evolved using the U matrix generated by the IM-SRG. Finally, all of the energies and the expectation values of any desired operators are printed out along with the estimated compute times of the various steps of the calculation, then the program exits, saving all of its progress to disk.

6.1 Harmonic Oscillator Basis Two-Body

In the harmonic oscillator basis, most of the code makes use of the existing framework built in the IM-SRG code [39]. The matrix elements are calculated using equation 3.28 and saved to disk using the ‘me2j’ file format. Originally developed at TU Darmstadt, it has since become a regularly used format in the nuclear physics community, as well as gaining use in quantum dot calculations [5]. These matrix elements are saved up to $E_{max} = 24$ on our compute cluster. Once saved to disk, it is computationally much faster to read them back in and scale the value of the harmonic oscillator as per equation 3.29.

The one-body components, the kinetic energy as well as the Coulomb interaction between the nucleus and the electrons, were calculated at run-time and typically required an insignificant amount of compute time.

6.2 Laguerre Basis Two-Body

In the Laguerre basis, a few pieces of code needed to be changed. For starters, since the harmonic oscillator and Laguerre bases use different definition of E_{max} , the number of orbits and the quantum numbers of said orbits had to be reworked slightly. Because this difference in the meaning of E_{max} and the number of orbits, the ‘me2j’ file format used in the harmonic oscillator basis could not be used immediately out of the box. For the simplicity of implementation, a new simpler file format was created which I have named ‘lv2’ format

(Livermore 2-body). Unlike the ‘me2j’ format, which has implicit quantum numbers, the ‘lv2’ file format explicitly lists the quantum numbers associated with a calculated matrix element. For example:

$$\langle (00\frac{1}{2})(01\frac{1}{2}) | O | (01\frac{3}{2})(10\frac{1}{2})1 \rangle = 1.234. \quad (6.1)$$

Where O simply designates some operator, and the value of this matrix is purely for illustrative purposes. This matrix element would be saved to file as:

```
0 0 1 0 1 1 0 1 3 1 0 1 1 1.234
```

Note that the j quantum numbers simply store the numerator since the denominator is always 2. Although this is an incredible verbose method of storing data, it is sufficient for the purposes of this thesis. Saving all of the matrix elements up to $E_{max} = 12$, for example, only used 5.7 GB of space, while the computers we used each have approximately 256 GB of RAM, and terabytes of hard disk space. More dense formats for could certainly be employed, but given the relatively small format of the existing data, it was not necessary to implement a more d format.

Chapter 7

Results and Discussion

In the following sections, the results of both the Laguerre and harmonic oscillator functions are discussed. The experimental values for the expectation values of the ground state energies are determined using the collected data from NIST. In the discussion of the harmonic oscillator we limit our discussion to the helium atom due to the computational complexity, and poor convergence associated with the harmonic oscillator basis functions. In the Laguerre basis, we are able to show calculations of helium, neon, argon, krypton, and xenon. It should be noted that experimental uncertainty in atomic ground-state energies is incredibly small, often on the order of part-per-million, and are thus insignificant as compared to the differences between Hartree-Fock and IM-SRG calculations.

7.1 Harmonic Oscillator Basis

Before evaluating the full many-body Schrödinger equation, we will first evaluate the harmonic oscillator basis in the one-body case to determine how well it is able to reproduce the interaction between electrons and the nucleus in the following toy-model Hamiltonian:

$$H = \sum_a^N T_a + \sum_a^N V_a. \quad (7.1)$$

Where N is the number of electrons. Assuming we are dealing with only two electrons with zero angular momentum, we know from basic quantum mechanics that the expected value

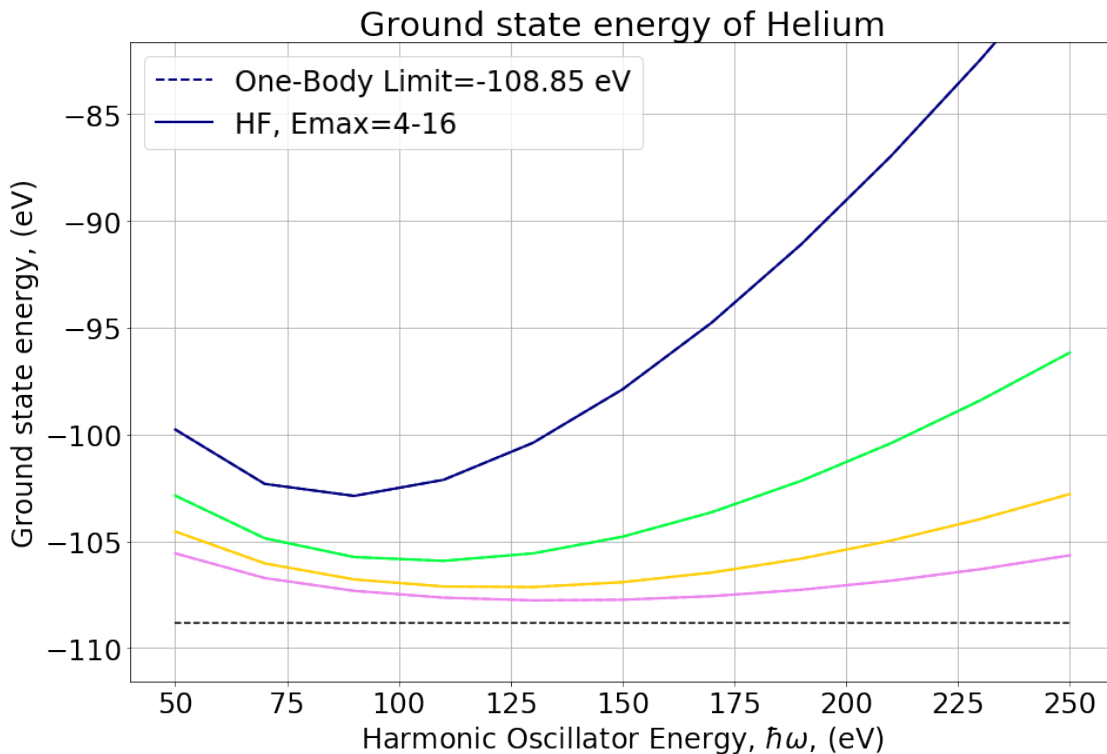


Figure 7.1: Expectation of the ground state energy of helium, omitting the interaction between electrons as a function of the harmonic oscillator energy, $\hbar\omega$, and the truncation parameter, E_{max} . Blue indicates the lowest E_{max} , at $E_{max}=4$, increasing in increments of 4 while purple indicates the highest, at $E_{max}=16$.

of the energy of this system is:

$$E = 2(-13.6 \text{ eV})Z^2 = -108.8 \text{ eV}. \quad (7.2)$$

Solving for this using only the Hartree-Fock method, we should see the expectation value converge to this value for some large enough value of E_{max} .

As E_{max} goes to large values in figure 7.1, it appears that the harmonic oscillator basis is able to reproduce the one-body energy in this toy model, however, it does appear to require a very large modelspace in order to accomplish this. In the limit of large E_{max} , we should see the function converge regardless of the value of $\hbar\omega$. If we select a particular value of $\hbar\omega$ and plot the energy as a function of the truncation parameter, we get figures 7.2 and 7.3.

Harmonic oscillator basis converges quite slowly with respect to E_{max} , so it is computationally unfeasible to get very much data. Figure 7.4 shows the result for both the

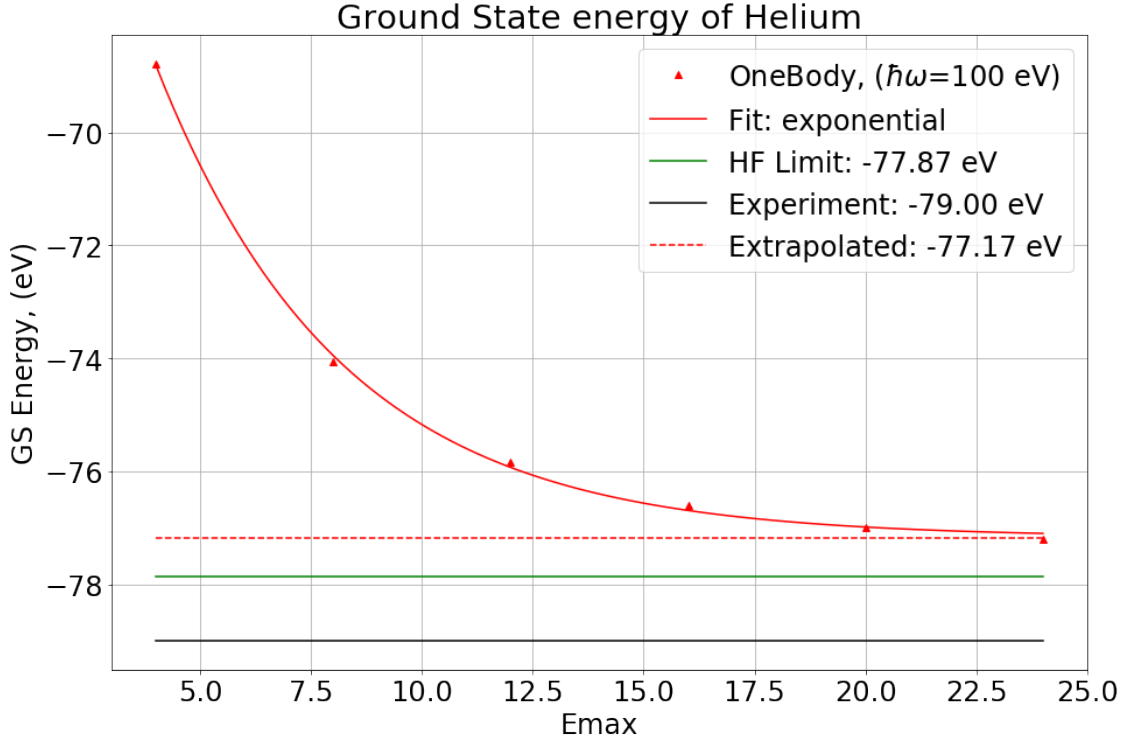


Figure 7.2: Expectation of the ground state energy of helium, omitting the interaction between electrons as a function of the truncation parameter, E_{max} , using an exponential fit.

Hartree-Fock energy using a Gaussian extrapolation as a function of the truncation parameter, E_{max} . Note that all of the calculations are done with a harmonic oscillator energy, $\hbar\omega$ of 100 eV. This number was chosen because it was near the energy where $E_{max} = 16$ was minimized and therefore likely a good starting point.

Using a Gaussian extrapolation (fig. 7.4), the extrapolated value after IM-SRG is -78.00 eV, and using exponential fit (fig. 7.5) the extrapolated value is -77.53 eV. By comparison the Hartree-Fock limit of helium is -77.87 eV [40]. For comparison the experimental value is $-79.0051538 \text{ eV} \pm 0.0000005 \text{ eV}$ [36]. Neither result is particularly promising, and the fact that the calculations, before extrapolation, have not even managed to exceed the Hartree-Fock limit motivated the change to new basis functions.

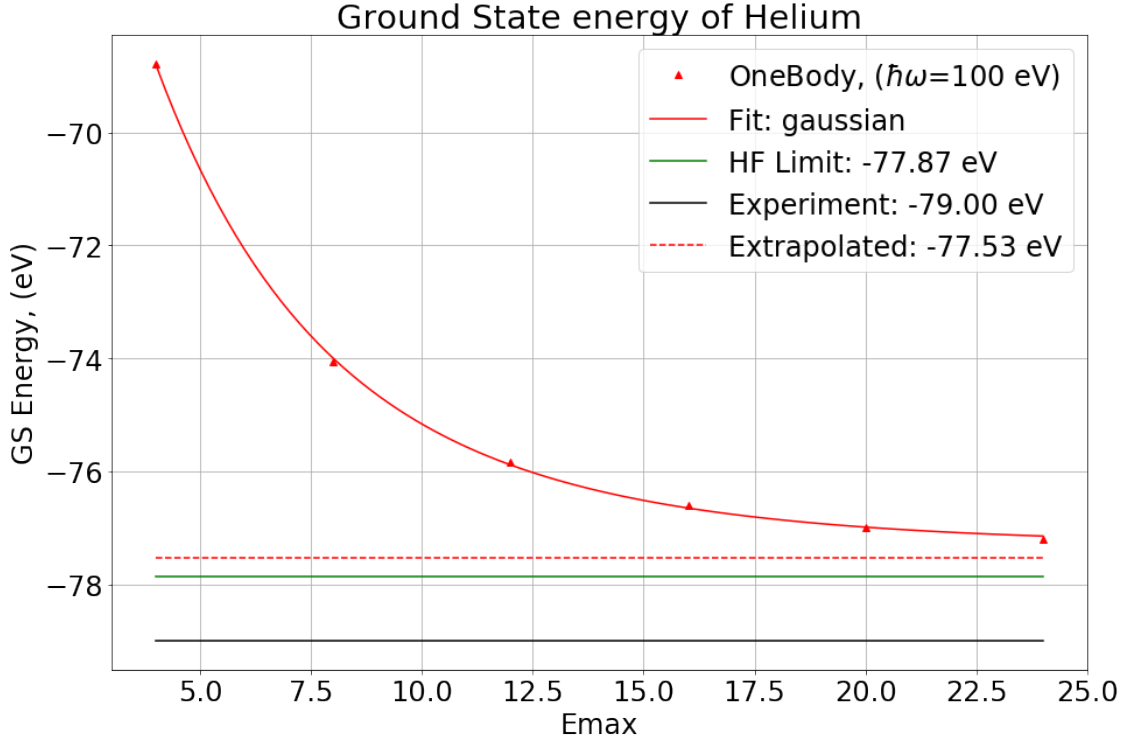


Figure 7.3: Expectation of the ground state energy of helium, omitting the interaction between electrons as a function of the truncation parameter, E_{max} , using a Gaussian fit.

7.2 Laguerre Basis

As with the harmonic oscillator case, we first evaluate the Laguerre basis functions in the simple Hamiltonian given by eqn. 7.1. Given that the results of eqn. 7.2 are independent of the choice of basis, we expect that the ground state energy in any basis should converge to -108.8 eV. As we can see in figure 7.6, the Laguerre basis is able to exactly reach the expected value of -108.8 eV, even with an extremely small modelspace. This indicates that this basis is likely a good choice for atomic calculations.

In fact, at $b = 2$, the Laguerre function exactly equals -108.8 eV; this is because for $b = 2$, neglecting the two-body interaction, the the Laguerre function reduces down to a hydrogen-like atom with $Z = 2$ and is an eigenfunction of this toy Hamiltonian. Thus we expect a single electron to be minimized as $b = 2$. Examining the region around $b = 2$, we can see that it is minimized at $b = 2$, and that it never goes below -108.8 eV, for $E_{max} = 2 - 6$ (see figures 7.6 and 7.7).

It is worth noting that as E_{max} tends towards very large (possibly infinite) numbers,

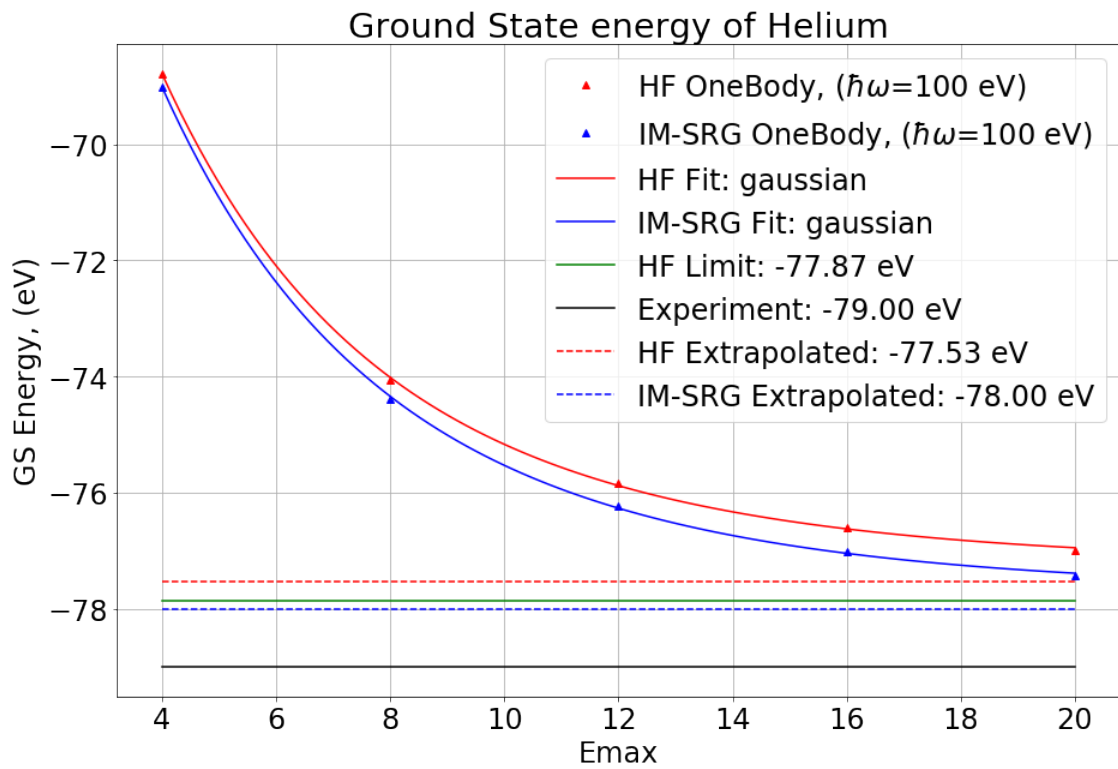


Figure 7.4: Gaussian extrapolation of the ground state energy of helium as a function of the truncation parameter, E_{max} .

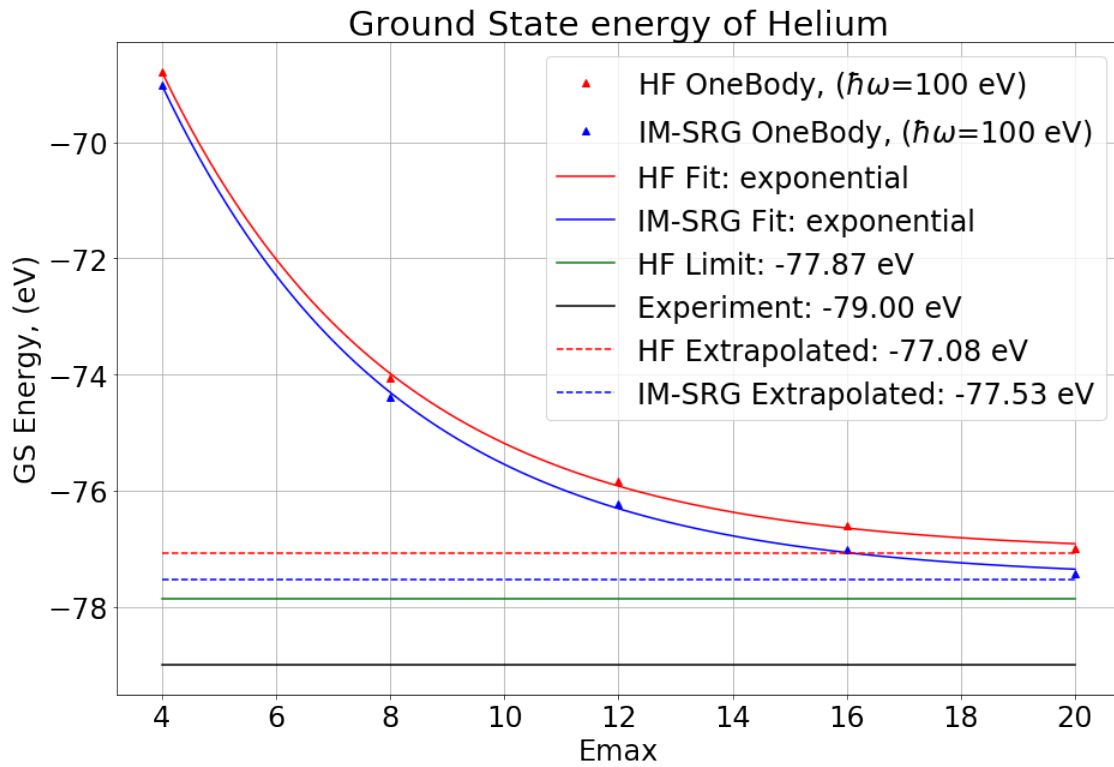


Figure 7.5: Exponential extrapolation of the ground state energy of helium as a function of the truncation parameter, E_{max} .

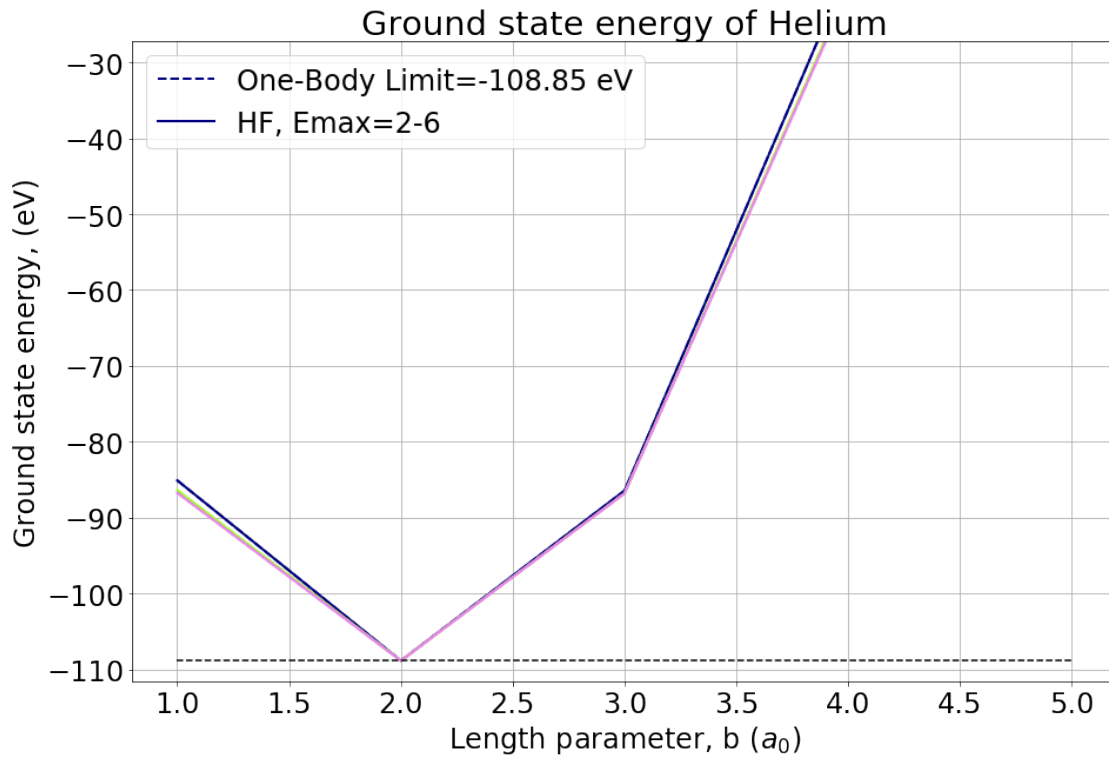


Figure 7.6: Expectation of the ground state energy of helium, omitting the interaction between electrons as a function of the length parameter, b and the truncation parameter, E_{max} , Blue indicates the lowest E_{max} , at $E_{max}=2$, increasing in increments of 2 while pink indicates the highest, at $E_{max}=6$.

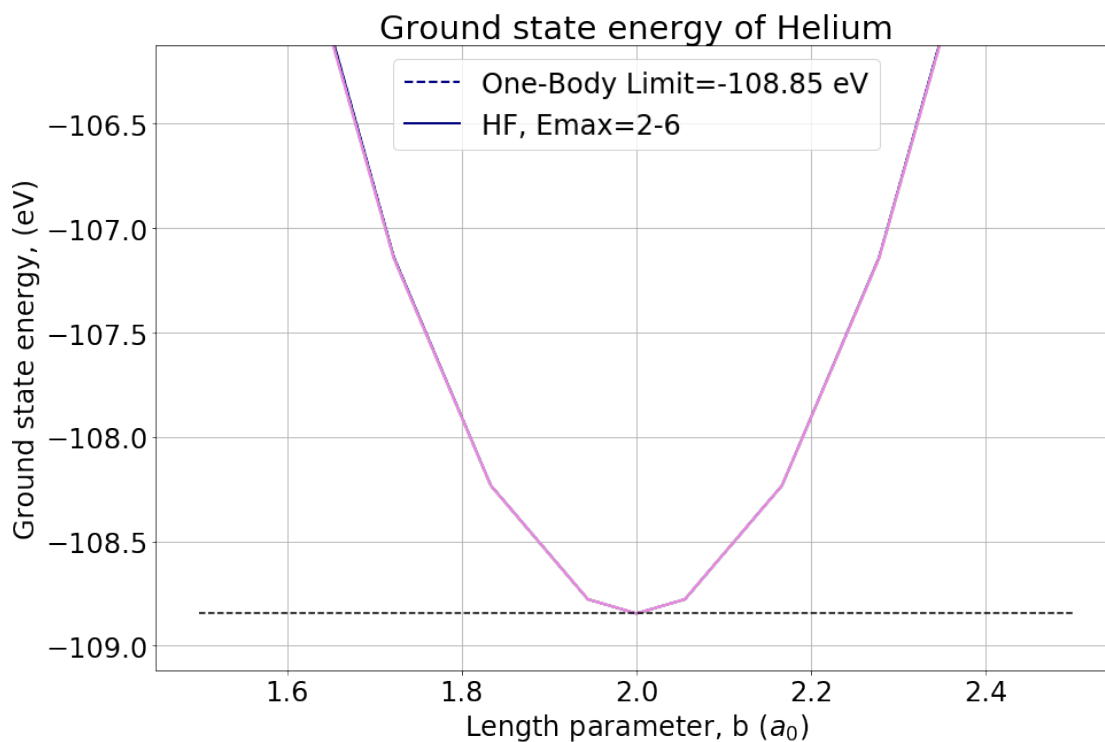


Figure 7.7: Expectation of the ground state energy of helium, omitting the interaction between electrons as a function of the length parameter, b and the truncation parameter, E_{max} ; examining the region about $b=2$, Blue indicates the lowest E_{max} , at $E_{max}=2$, increasing in increments of 2 while pink indicates the highest, at $E_{max}=6$.

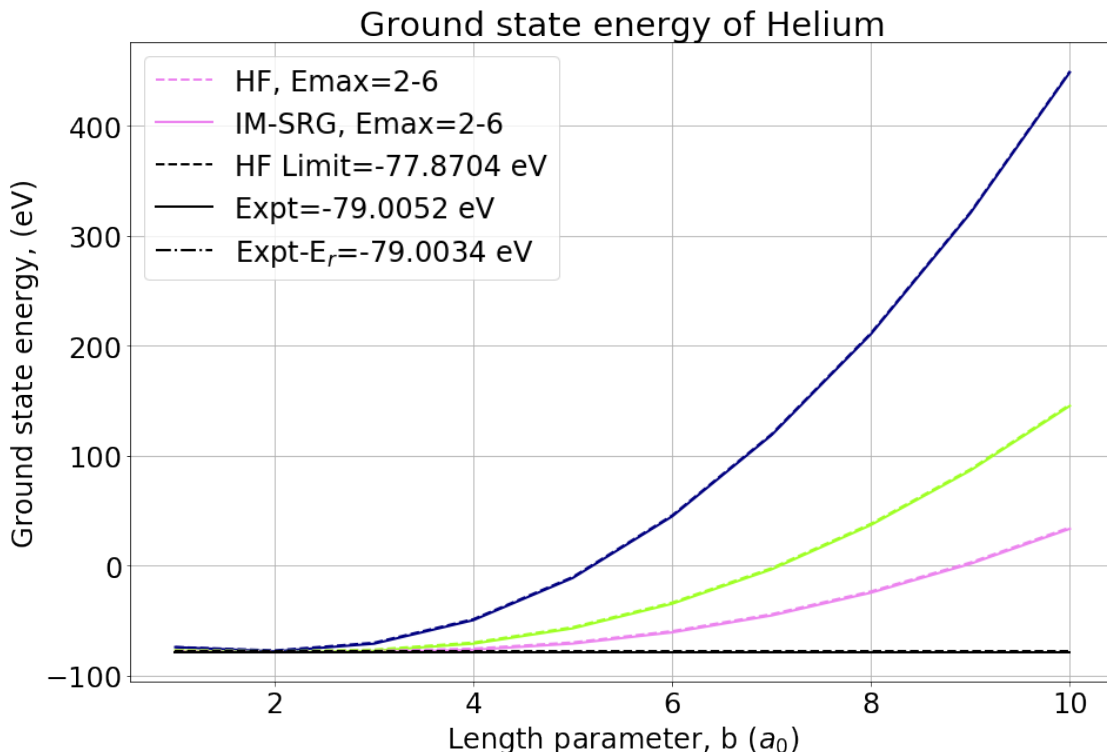


Figure 7.8: Hartree-Fock and IM-SRG calculations of the ground state of helium as a function of the truncation parameter, E_{max} , and the length parameter, b , including the Coulomb interaction between the electrons. Blue indicates the lowest E_{max} , at $E_{max}=2$, increasing in increments of 2 while pink indicates the highest, at $E_{max}=6$.

we expect the curves as a function of b to flatten out and approach the experimental or Hartree-Fock curves, respectively, which is the trend we see in figures 7.8, 7.9, 7.10, 7.11, 7.12, 7.13.

Including the interaction between the electrons, and solving for the full Hamiltonian given by equations 2.1, we attempt to solve for the ground state energy of helium. In figure 7.8, we may examine the convergence of the Laguerre basis in solving the helium Hamiltonian from $E_{max} = 2 - 6$. In figures 7.8-7.13, the experimental values, (Expt) listed are listed from NIST [36], Hartree-Fock limits from [40], and the relativistic energy, E_r , from [40].

Even at $E_{max} = 6$, the Hartree-Fock calculation agrees closely with literature values, and the IM-SRG value at $b = 2$ is -79.001 eV agrees with experimental value to within 0.05%. Evaluating helium in the region around $b = 2$ up to $E_{max} = 12$, we can see that this basis has excellent convergence, (fig. 7.9). At the minima at $E_{max} = 12$, the calculated ground state energy is -79.015 eV which deviates from the experimental value by 0.015%;

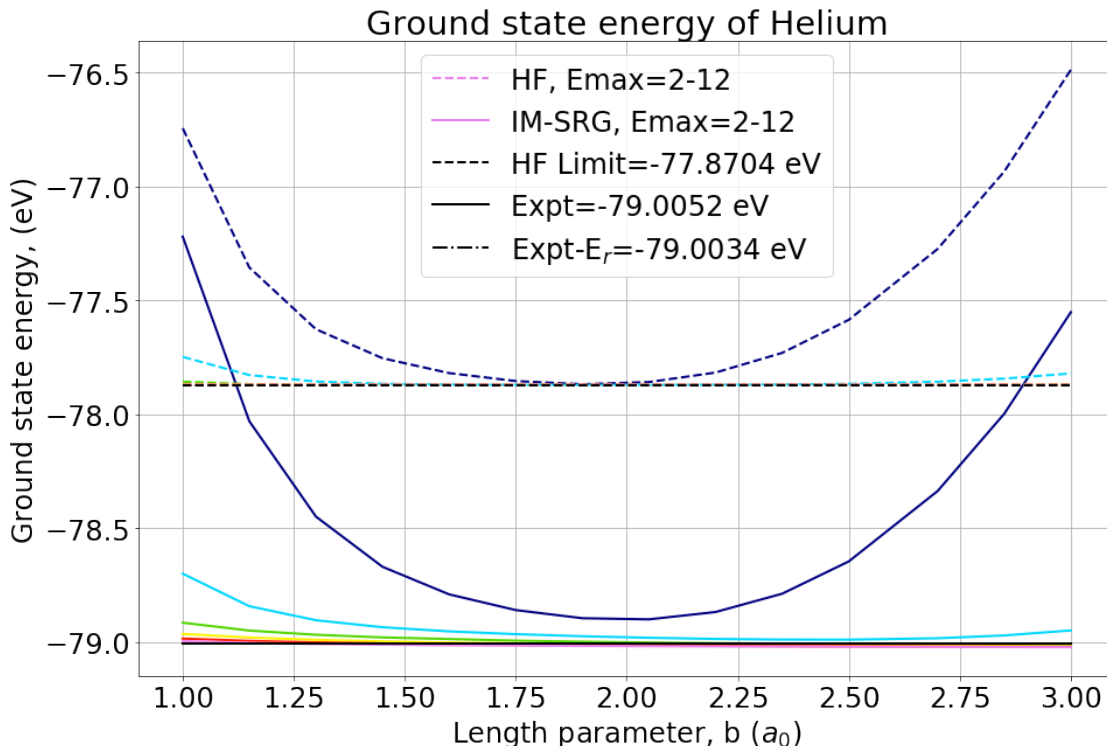


Figure 7.9: Hartree-Fock and IM-SRG calculations of the ground state of helium as a function of the truncation parameter, E_{max} , and the length parameter, b , including the Coulomb interaction between the electrons examining the region around $b=2$. Dark blue indicates $E_{max}=2$, cyan is $E_{max}=4$, increasing in increments of 2, with purple being the highest at $E_{max}=12$.

large compared to the experimental uncertainty of 5×10^{-7} eV. Although this value is lower than the experimental value, and thus violates the variation principle as described in section 4.1.1, however the numerical integration was performed with an uncertainty of about 1 part in 10^{-3} , and the Hamiltonian used is omitting higher order effects, such as relativistic and magnetic interactions[10]. Note that the values at large E_{max} are so close that extrapolated values do not deviate meaningfully from the rigorously calculated values.

Evaluating the ground state of neon, the next closed-shell atom, we can see that although the Laguerre basis appears to reproduce the Hartree-Fock limit, the IM-SRG value appears to reach the experimental value. Figure 7.10 shows that the calculation is able to reach the Hartree-Fock limit, even around $E_{max} = 8$, and the calculation appears to approach the experimental limit. One of the other dominant contributions in the atomic Hamiltonian are the relativistic effects, which are neglected in this work. Desclaux has made a comprehensive

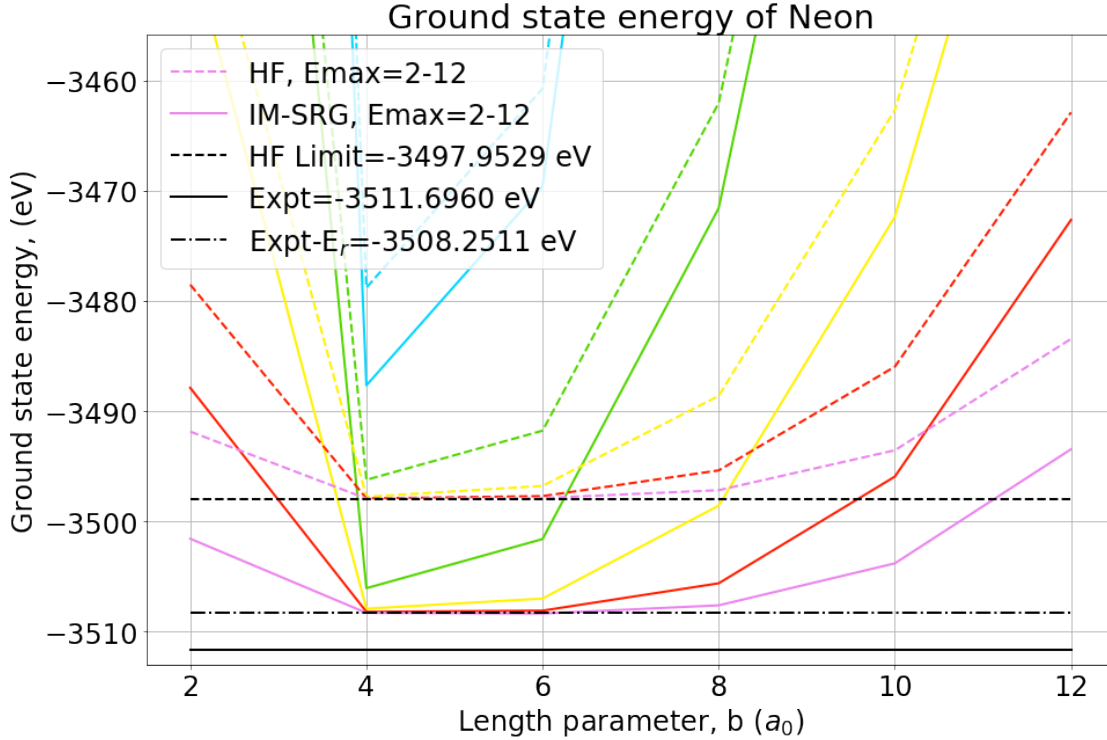


Figure 7.10: Hartree-Fock and IM-SRG calculations of the ground state of Neon as a function of the truncation parameter, E_{max} , and the length parameter, b . Dark blue indicates $E_{max}=2$, cyan is $E_{max}=4$, increasing in increments of 2, with purple being the highest at $E_{max}=12$.

calculation of the relativistic corrections for uncharged for elements from $Z = 1 - 120$ by numerically solving the Dirac equation, and the corrections for small elements is extraordinarily small [10]. Helium, for example has a correction of approximately 0.0003 eV, while for Neon the correction is about 3 eV or less than 0.1% of the ground state energy, but for xenon, the difference is on the order of 5.4 keV, or about 3% of the ground state energy.

In figures 7.9-7.13, the values with the dot-dash-dot line represent the experimental value, minus the estimated relativistic energy from [10]. For helium, the relativistic energy is negligible as compared to the Hartree-Fock energy. However, for atoms with larger proton number, the relativistic energy dominates. IM-SRG is designed specifically with the idea of accounting for the correlation energy, other corrections such as relativistic effects must be taken into account by creating relativistic operators and evolving them the same as one would evolve non-relativistic operators.

In figures 7.12-7.13, the reader may notice that a number of datapoints are missing, these

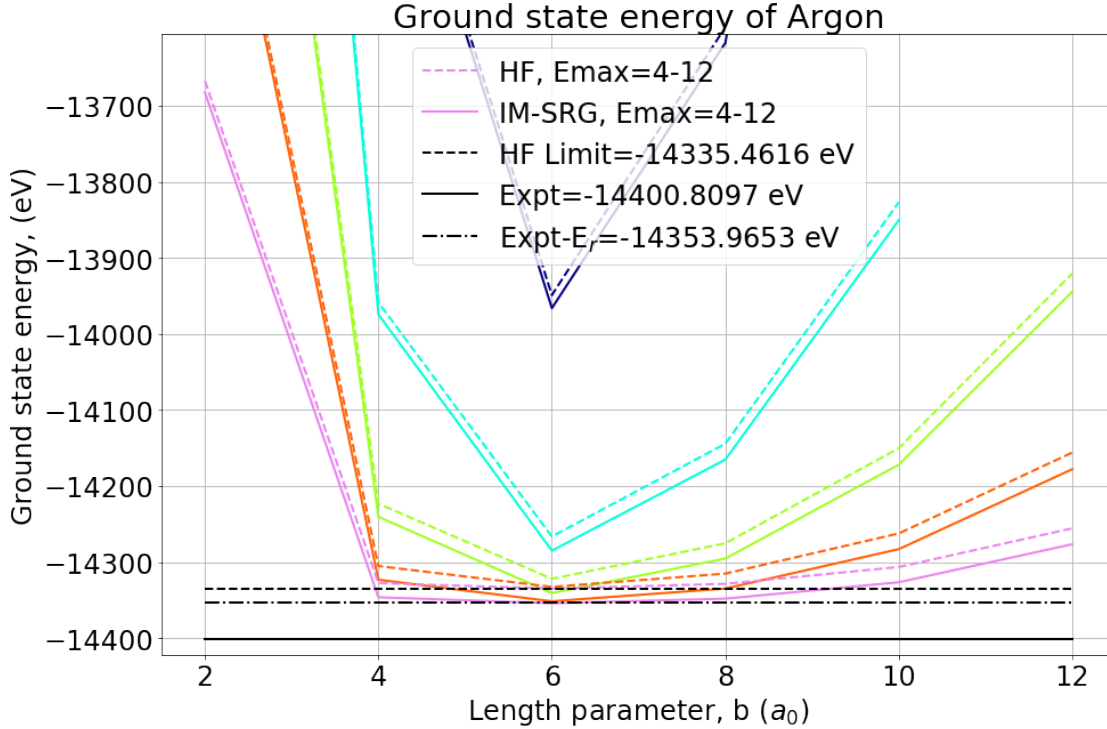


Figure 7.11: Hartree-Fock and IM-SRG calculations of the ground state of argon as a function of the truncation parameter, E_{max} , and the length parameter, b . Dark blue indicates $E_{max}=2$, cyan is $E_{max}=4$, increasing in increments of 2, with purple being the highest at $E_{max}=12$.

points were omitted either because they were not needed to demonstrate the trend, or in the case of the xenon figure (fig 7.13), these were calculations that hit the time limit of the compute cluster without finishing. Although more compute time can be requested, these calculations already take many hours and may require tens of hours to complete, which is difficult to justify given the trend set by previous calculations.

The reader should note that in the calculations of helium, neon, argon and krypton, the difference in E_{max} from one calculation to the next was 2, but in xenon it was only 1, in order to better demonstrate the trend.

The table below is a summary of the calculated ground state energies for helium, neon, argon, krypton, and xenon.

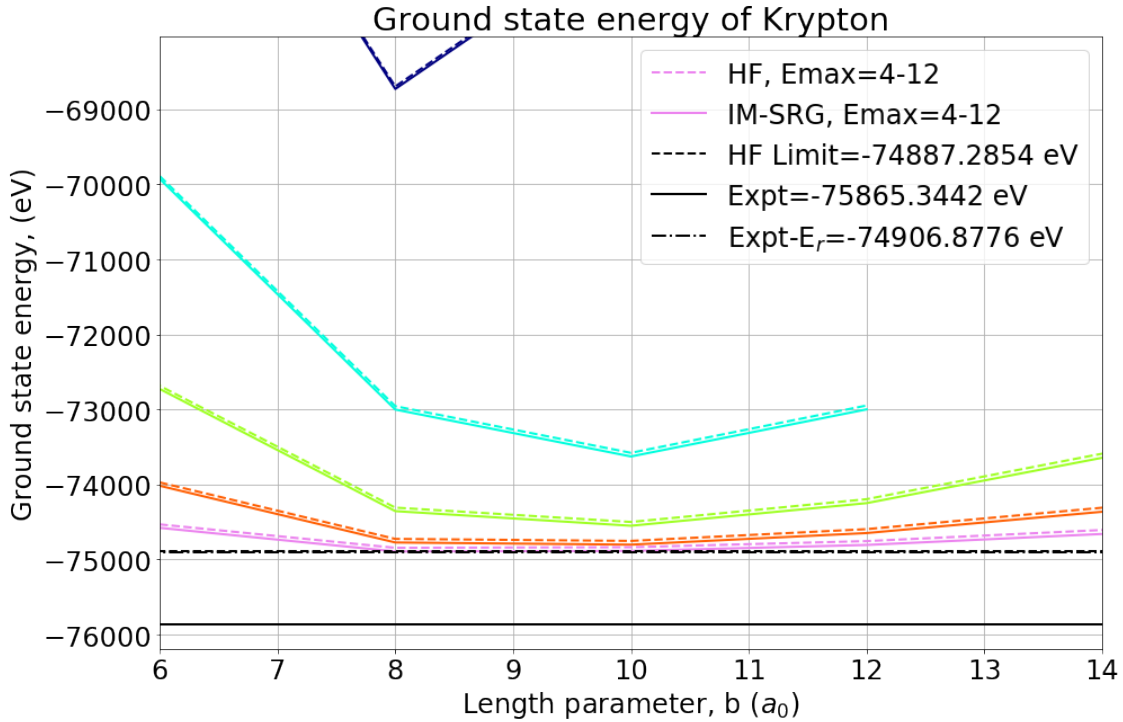


Figure 7.12: Hartree-Fock and IM-SRG calculations of the ground state of krypton as a function of the truncation parameter, E_{max} , and the length parameter, b . Dark blue indicates $E_{max}=2$, cyan is $E_{max}=4$, increasing in increments of 2, with purple being the highest at $E_{max}=12$.

Table 7.1: Summary of the Results of the IM-SRG Calculations, comparing the results to the Hartree-Fock Limit, Experimental Results minus Relativistic Energy, and Experimental Results

Element	HF Limit	IM-SRG	Expt- E_r	Expt
helium	-77.870 eV	-79.015 eV	-79.003 eV	-79.005 eV
neon	-3498.0 eV	-3508.4 eV	-3508.3 eV	-3511.7 eV
argon	-13.335 keV	-14.354 keV	-14.353 keV	-14.400 keV
krypton	-74.887 keV	-74.892 keV	-74.906 keV	-75.865 keV
xenon	-196.80 keV	195.95 keV	-196.73 keV	-202.40 keV

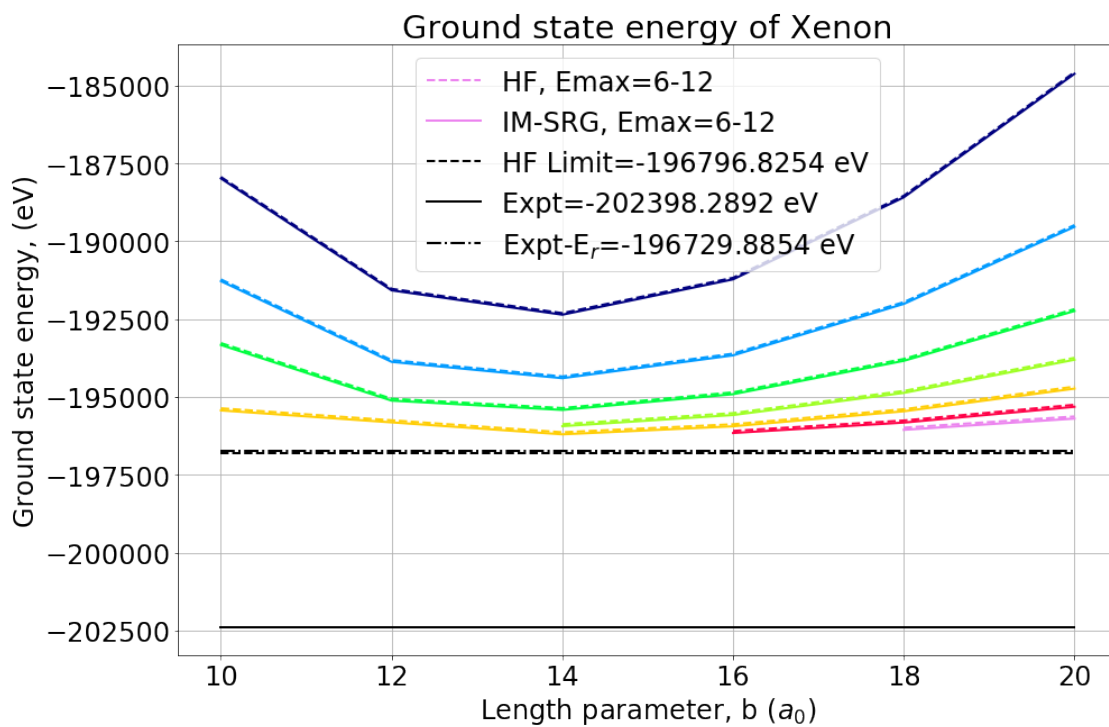


Figure 7.13: Hartree-Fock and IM-SRG calculations of the ground state of xenon as a function of the truncation parameter, E_{max} , and the length parameter, b . Dark blue indicates $E_{max}=2$, cyan is $E_{max}=4$, increasing in increments of 2, with purple being the highest at $E_{max}=12$.

Chapter 8

Conclusion & Future Work

In conclusion, we demonstrate that the Laguerre basis functions provide an excellent set of basis functions for the atomic many-body Hamiltonian for the IM-SRG method is an excellent post-Hartree-Fock method for determining ground state energies of the first five noble gases, neglecting relativistic effects. For this reason, it may be that in computational chemistry using light elements may find IM-SRG to be a useful post-Hartree-Fock tool.

For elements with open shells, such as lithium or carbon, I am planning to use a computational tool known as NuShell in order to calculate the ground state properties [41]. Developed at University of Oxford and Michigan State University, NuShell has become a popular tool in the nuclear physics community, but in principle, I believe it would not be difficult to use it without any modification to the NuShell code to determine the ground state energies. Work is already underway to use NuShell to calculate the ground state energies lithium and carbon. Preliminary results for lithium appear promising, however the results were not ready in time to include in this thesis.

If elements heavier than neon, are to be calculated, it will be necessary to incorporate relativistic effects, but for lighter atoms one may certainly achieve good post-Hartree-Fock results without too much modification. The relativistic interaction in atomic physics is well-known, in fact entire textbooks have been written on the matter [42].

Although the main purpose of this thesis has been accomplished there are still several promising routes for this research to progress and the need for further research is required.

Bibliography

- [1] H. Hergert, S. Bogner, T. Morris, A. Schwenk, and K. Tsukiyama, “The in-medium similarity renormalization group: A novel ab initio method for nuclei,” *Physics Reports*, vol. 621, p. 165–222, Mar 2016.
- [2] H. Hergert, J. M. Yao, T. D. Morris, N. M. Parzuchowski, S. K. Bogner, and J. Engel, “Nuclear structure from the in-medium similarity renormalization group,” *Journal of Physics: Conference Series*, vol. 1041, p. 012007, May 2018.
- [3] H. Hergert, S. K. Bogner, J. G. Lietz, T. D. Morris, S. Novario, N. M. Parzuchowski, and F. Yuan, *In-Medium Similarity Renormalization Group Approach to the Nuclear Many-Body Problem*, ch. 10, pp. 477–570. Springer, 2017.
- [4] N. M. Parzuchowski, T. D. Morris, and S. K. Bogner, “Ab initio excited states from the in-medium similarity renormalization group,” *Physical Review C*, vol. 95, p. 044304, Apr 2017.
- [5] F. Yuan, S. J. Novario, N. M. Parzuchowski, S. Reimann, S. K. Bogner, and M. Hjorth-Jensen, “Addition and removal energies of circular quantum dots,” *The Journal of Chemical Physics*, vol. 147, p. 164109, Nov 2017.
- [6] G. W. Drake, W. Nörtershäuser, and Z.-C. Yan, “Isotope shifts and nuclear radius measurements for helium and lithium,” *Canadian Journal of Physics*, vol. 83, no. 4, pp. 311–325, 2005.

- [7] S. Zerguine, P. Van Isacker, A. Bouldjedri, and S. Heinze, “Correlating radii and electric monopole transitions of atomic nuclei,” *Physical Review Letters*, vol. 101, no. 2, p. 022502, 2008.
- [8] A. C. Mueller, F. Buchinger, W. Klempt, E. Otten, R. Neugart, C. Ekström, and J. Heinemeier, “Spins, moments and charge radii of barium isotopes in the range $^{122-146}\text{Ba}$ determined by collinear fast-beam laser spectroscopy,” *Nuclear Physics A*, vol. 403, no. 2, pp. 234–262, 1983.
- [9] D. J. Griffiths, *Introduction to Quantum Mechanics*. Prentice Hall, 1995.
- [10] J. Desclaux, “Relativistic Dirac-Fock expectation values for atoms with $Z=1$ to $Z=120$,” *Atomic data and nuclear data tables*, vol. 12, no. 4, pp. 311–406, 1973.
- [11] E. A. Hylleraas, “The Schrödinger two-electron atomic problem,” in *Advances in Quantum Chemistry*, vol. 1, pp. 1–33, Elsevier, 1964.
- [12] P. Manninen, “Lecture notes for the course 554017 advanced computational chemistry.” http://www.chem.helsinki.fi/~manninen/lecture_notes.pdf, 2009.
- [13] P. L. Fast, M. L. Sánchez, and D. G. Truhlar, “Infinite basis limits in electronic structure theory,” *The Journal of chemical physics*, vol. 111, no. 7, pp. 2921–2926, 1999.
- [14] A. Sandulescu, H. Scutaru, and W. Scheid, “Open quantum system of two coupled harmonic oscillators for application in deep inelastic heavy ion collisions,” *Journal of Physics A: Mathematical and General*, vol. 20, no. 8, p. 2121, 1987.
- [15] D. J. Rowe, “The harmonic oscillator and nuclear physics,” in *Workshop on Harmonic Oscillators* (D. Han, Y. S. Kim, and W. W. Zachary, eds.), NASA, 1993.
- [16] J. Suhonen, *From Nucleons to Nucleus*. Springer, 2007.
- [17] A. McCoy and M. Caprio, “Algebraic evaluation of matrix elements in the laguerre function basis,” *Journal of Mathematical Physics*, vol. 57, no. 2, p. 021708, 2016.
- [18] M. Rotenberg, “Theory and application of sturmian functions,” in *Advances in Atomic and Molecular Physics*, vol. 6, pp. 233–268, Elsevier, 1970.

- [19] R. S. Mulliken, “Electronic population analysis on LCAO-MO molecular wave functions. I,” *The Journal of Chemical Physics*, vol. 23, no. 10, pp. 1833–1840, 1955.
- [20] A. Brown, “Lecture notes in nuclear structure theory.” <https://people.nslc.msu.edu/~brown/Jina-workshop/BAB-lecture-notes.pdf>, November 2005.
- [21] E. Weisstein, “Wigner 9j-symbol.” <http://mathworld.wolfram.com/Wigner9j-Symbol.html>, Apr 2019.
- [22] E. W. Weisstein, “Wigner-Eckhart theorem.” <http://mathworld.wolfram.com/Wigner-EckartTheorem.html>, Jul 2019.
- [23] S. G. Johnson, “Cubature.” <https://github.com/stevengj/cubature>, Aug 2018.
- [24] M. Caprio, P. Maris, and J. Vary, “Coulomb-Sturmian basis for the nuclear many-body problem,” *Physical Review C*, vol. 86, no. 3, p. 034312, 2012.
- [25] M. Moshinsky, “Transformation brackets for harmonic oscillator functions,” *Nuclear Physics*, vol. 13, p. 104–116, May 1959.
- [26] J. C. Slater, “A Simplification of the Hartree-Fock Method,” *Physical Review*, vol. 81, no. 3, p. 385, 1951.
- [27] F. Jensen, *Introduction to computational chemistry*. John Wiley & Sons, 2017.
- [28] F. Wegner, “Flow equations for Hamiltonians,” *Advances in Solid State Physics Advances in Solid State Physics 40*, p. 133–142, 2000.
- [29] M. Hjorth-Jensen, M.-P. Lombardo, and U. v. Kolck, *An Advanced Course in Computational Nuclear Physics: Bridging the Scales from Quarks to Neutron Stars*. Springer, 2017.
- [30] L. G. Molinari, “Notes on Wick’s Theorem in Many-Body Theory,” *arXiv preprint arXiv:1710.09248*, 2017.
- [31] K. Tsukiyama, S. K. Bogner, and A. Schwenk, “In-medium similarity renormalization group for nuclei,” *Physical Review Letters*, vol. 106, no. 22, p. 222502, 2011.

- [32] K. Tsukiyama, S. K. Bogner, and A. Schwenk, “In-medium similarity renormalization group for open-shell nuclei,” *Physical Review C*, vol. 85, no. 6, p. 061304, 2012.
- [33] V. Vasilyev, “Online complete basis set limit extrapolation calculator,” *Computational and Theoretical Chemistry*, vol. 1115, pp. 1–3, 2017.
- [34] E. W. Weisstein, “Least squares fitting.” <http://mathworld.wolfram.com/LeastSquaresFitting.html>, Apr 2019.
- [35] A. Varandas, “Extrapolation to the complete-basis-set limit and the implications of avoided crossings: The $X^1\Sigma_g^+$, $B^1\Delta_g$, and $B^1\Sigma_g^+$ states of C_2 ,” *The Journal of Chemical Physics*, vol. 129, no. 23, p. 234103, 2008.
- [36] A. Kramida, Yu. Ralchenko, J. Reader, and and NIST ASD Team. NIST Atomic Spectra Database(ver. 5.6.1), [Online]. Available: <https://physics.nist.gov/asd> [2019, May 15]. National Institute of Standards and Technology, Gaithersburg, MD., 2018.
- [37] G. A. Negoita, G. R. Luecke, J. P. Vary, P. Maris, A. M. Shirokov, I. J. Shin, Y. Kim, E. G. Ng, and C. Yang, “Deep learning: a tool for computational nuclear physics,” *arXiv preprint arXiv:1803.03215*, 2018.
- [38] G. A. Negoita, J. P. Vary, G. R. Luecke, P. Maris, A. M. Shirokov, I. J. Shin, Y. Kim, E. G. Ng, C. Yang, M. Lockner, *et al.*, “Deep learning: Extrapolation tool for ab initio nuclear theory,” *arXiv preprint arXiv:1810.04009*, 2018.
- [39] H. H. Ragnar Stroberg, Koshiroh Tsukiyama and N. Parzuchowski, “*ragnar_imsrg*.” <https://github.com/ragnarstroberg/imsrg>, 2019.
- [40] C. F. Fischer, “Average-energy-of-configuration hartree-fock results for the atoms helium to radon,” *Atom. Data Nucl. Data Tabl.*, vol. 12, pp. 301–399, 1972.
- [41] B. Brown and W. Rae, “The shell-model code NuShellX@MSU,” *Nuclear Data Sheets*, vol. 120, pp. 115–118, 2014.
- [42] I. Grant, “Relativistic atomic structure,” *Springer Handbook of Atomic, Molecular, and Optical Physics*, pp. 325–357, 2006.